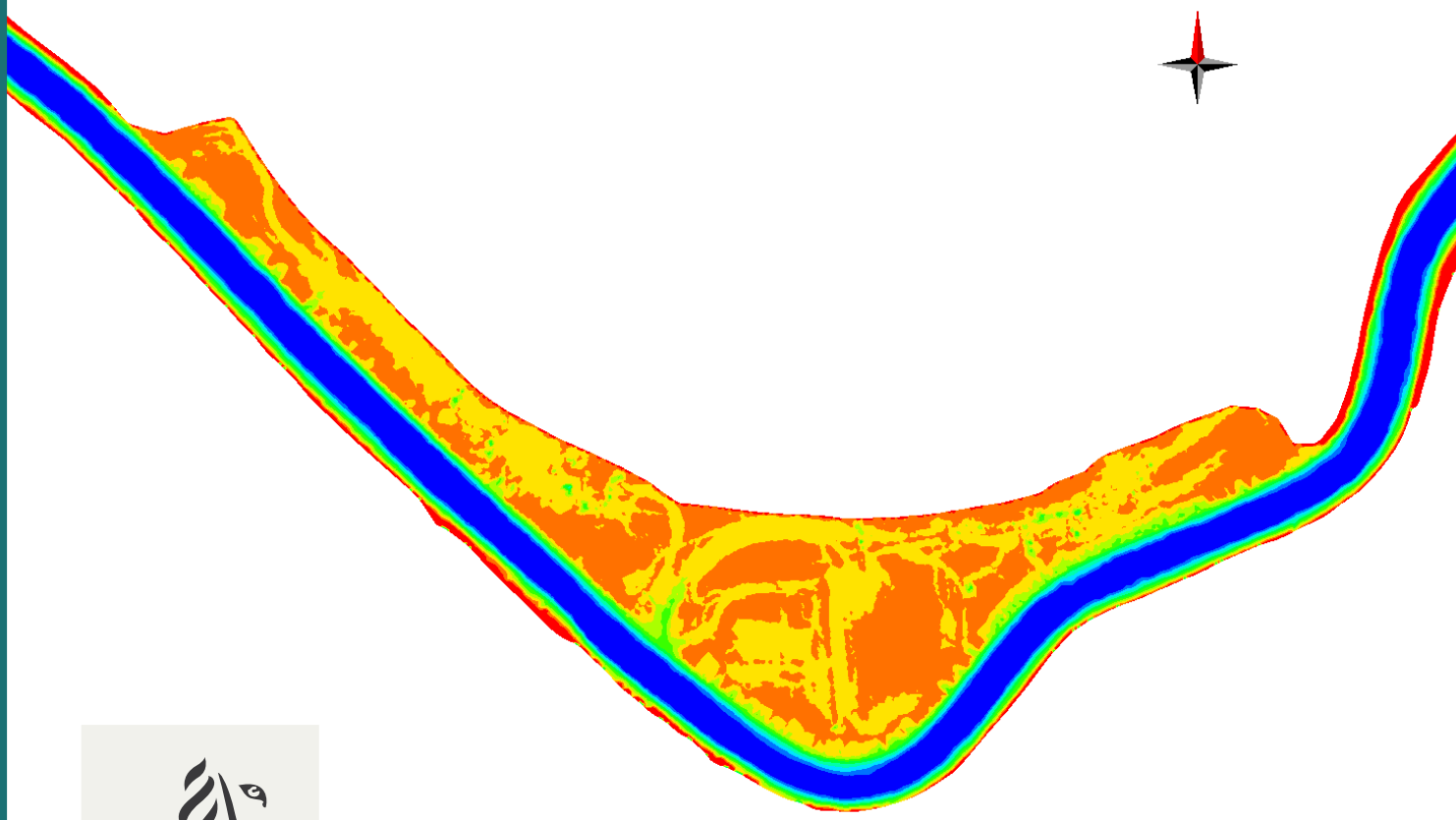

Flanders
State of the Art

18_138_1
FHR reports

A new ebb-flood channel system in the Upper Sea Scheldt (Wijmeers)

A model study with Telemac-3D

DEPARTMENT
MOBILITY &
PUBLIC
WORKS

www.flandershydraulicsresearch.be

A new ebb-flood channel system in the Upper Sea Scheldt (Wijmeers)

A model study with Telemac-3D

Bi, Q.; Smolders, S.; Vanlede, J.; Mostaert, F.

Flanders Hydraulics Research
Flanders State of the Art

Cover figure © The Government of Flanders, Department of Mobility and Public Works, Flanders Hydraulics Research

Legal notice

Copyright and citation

This publication should be cited as follows:

Bi, Q.; Smolders, S.; Vanlede, J.; Mostaert, F. (2019). A new ebb-flood channel system in the Upper Sea Scheldt (Wijmeers): A model study with Telemac-3D. Version 3.0. FHR Reports, 18_138_1. Flanders Hydraulics Research: Antwerp.

Document identification

Customer:	De Vlaamse Waterweg nv – Afd. Zeeschelde & Zeekanaal	Ref.:	WL2019R18_138_1
Keywords (3-5):	TELEMAC-3D, numerical modeling, ebb-flood system, Upper Sea Scheldt		
Text (p.):	53	Appendices (p.):	5
Confidentiality:	☒ No	☒ Available online	

Author(s):	Bi, Qilong

Control

	Name	Signature
Reviser(s):	Smolders, S.	Getekend door: Sven Smolders (Signature) Getekend op: 2019-09-03 12:36:39 +01:00 Reden: Ik keur dit document goed Sven Smolders
Project leader:	Vanlede, J.	Getekend door: Joris Vanlede (Signature) Getekend op: 2019-09-04 14:18:16 +01:00 Reden: Ik keur dit document goed Joris Vanlede

Approval

Head of Division:	Mostaert, F.	Getekend door: Frank Mostaert (Signature) Getekend op: 2019-09-03 11:25:32 +01:00 Reden: Ik keur dit document goed Frank Mostaert

Abstract

In this study, a 3D detailed hydrodynamic model is developed in TELEMAC, based on a cut-out from the calibrated SCALDIS model. The model is used to investigate the effects of different alternatives of a new ebb-flood channel system that is planned in the Upper Sea Scheldt at Wijmeers. Moreover, the stability of the secondary channels is evaluated.

Contents

List of tables

List of figures

1 Introduction

The ebb-flood channel system naturally exists in the Scheldt estuary. They form certain patterns and continue to evolve under tidal currents. They usually have significant influences on hydrodynamics, residual sediment transport in the estuary, and play important roles in many ecological aspects.

The ebb-flood channel system consists of two types of channels: a flood channel (in Dutch: 'vloedschaar') defined as a tidal channel that is open to the flood current and that exhibits a sill at the upstream end; and an ebb channel ('ebschaar') defined as a tidal channel that is primarily open to the ebb current and that exhibits a sill at the seaward end. Ebb and flood use different tidal channels in an estuary and form certain patterns to lead these different tides through (van Veen, 1950).

The following section is abbreviated from the theoretical background section in IMDC (2019, in prep)

1.1 Channel patterns in an estuary

The ebb and flood channels can be distinguished depending on the direction of net transport of sediment. Due to the dominance of ebb or flood tide in different channels, a residual flux can occur for each tidal cycle.

A system of ebb-flood channels can be understood from the three main aspects: tidal prism, meandering and sand transport. Tidal prism is considered as the primary driving force, but meandering is the phenomenon which determines the channel orientation and evolution. In addition, wind direction (wave action at the upwind side) and near-bank turbulence should also be taken into account in some cases (van Veen, 1950).

Robinson (1960) summarized three main patterns of the ebb-flood channels, in which, the flood and ebb channels are quite distinct and are separated by a shallower sill or bar (Figure 1).

Figure 1 – Various patterns of the mutual evasion of the ebb and flood channels.
1-Parallel, 2-Snake tongue, 3- Flank (Robinson, 1960)

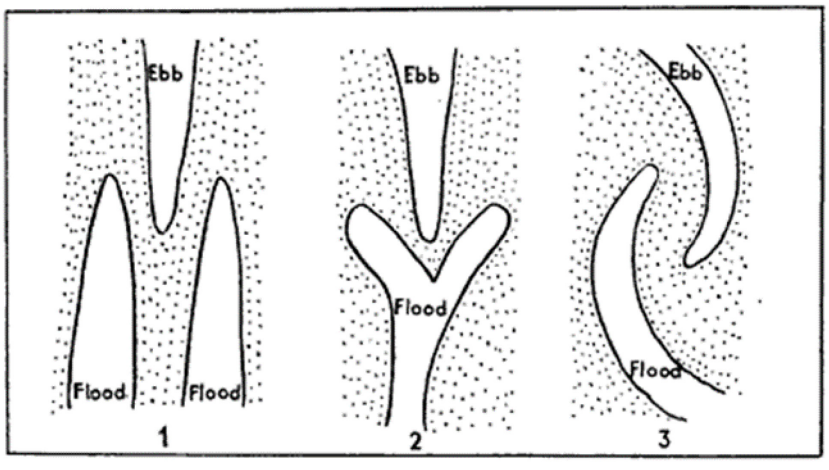

The pattern of the ebb and flood channels displays a close relationship to the shape and situation of the estuary. When the estuary is long and narrow and the amount of river water in circulation is considerable, e.g. Scheldt estuary, the ebb channel may be the dominant element in the bottom configuration. In such a situation the flood stream creates a number of short bars running into the bordering sand and mud flats at points where the ebb channel changes direction (Robinson, 1960).

Figure 2 – Sketch of an ideal system of ebb and flood channels at Scheldt estuary.
Main (ebb) channel, flood channels starting in each bend (Van Veen, 1950).

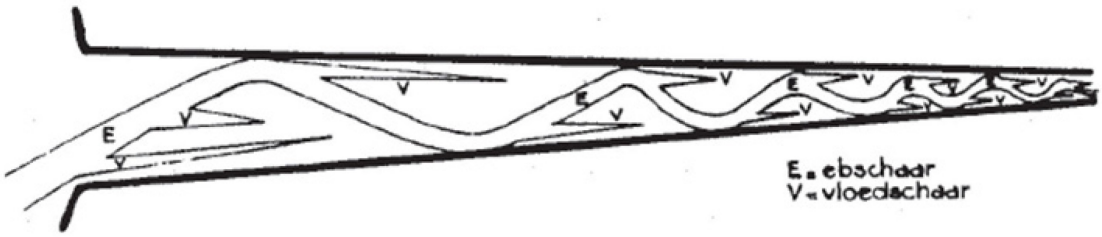

This is also pointed out by Van Veen (1950) that a meandering main ebb channel will develop if the width between the fixed banks is not too large. The flats in each inner bend will develop a flood channel, which have a double function: filling the tidal sand-flat in the inner bend of the main channel and serving the cut-off currents of the bend (Figure 2).

1.2 Channel patterns in tidally affected rivers

In tidally affected rivers, bifurcations tend to become unstable after certain period, as water will mainly flow through one channel, which is usually much larger than the other, abandoning the other and the remaining channel will eventually form a new bifurcation, repeating the process hereafter. This process generates ebb-flood channels in tidally affected rivers

The stability of the bifurcation is dependent on the width/depth ratio (Kleinhans & van den Berg, 2011). A relatively narrow and deep river with a low width-depth ratio is capable of moving more suspended sediment, but a more shallow and wider channel, with a larger width-depth ratio, is more efficient to transport bed load by shear on the bottom of the stream (Coleman, 1969). Moreover, the width-depth ratio changes continuously with the discharge, load type and slope of the bed.

Another important aspect in the formation of channels in the river is the turbulence. River flow is usually turbulent flow. The turbulent energy is responsible for entrainment of suspended sediment in the flow and it also affects the deposition of sediment. With different cross-section shape, the size of the belts and zones with different turbulence intensity shift laterally and vertically, which could lead to the formation of different channel patterns (Maity & Maiti, 2017).

1.3 Secondary channels

Secondary channels are river branches with their inlet and outflow connected to the main channel. These channels can exhibit instability in horizontal direction (meandering) and in vertical direction (aggradation or degradation).

Bank erosion determines the horizontal stability of the secondary channel (Barneveld et al., 1994). It mainly takes place in the outer bends of the secondary channel. The critical flow velocity is an important parameter for bank erosion. According to Schropp (1995), flow velocities have to be low enough to prevent erosion of the bed and bank erosion, but still high enough to satisfy the ecological targets, preferably covering the entire range of 0.10-0.80 m/s.

Figure 3 – Sediment distribution at bifurcations (Akkerman, 1993).
Q is the discharge in m^3/s and S is the sediment transport in m^3/s.

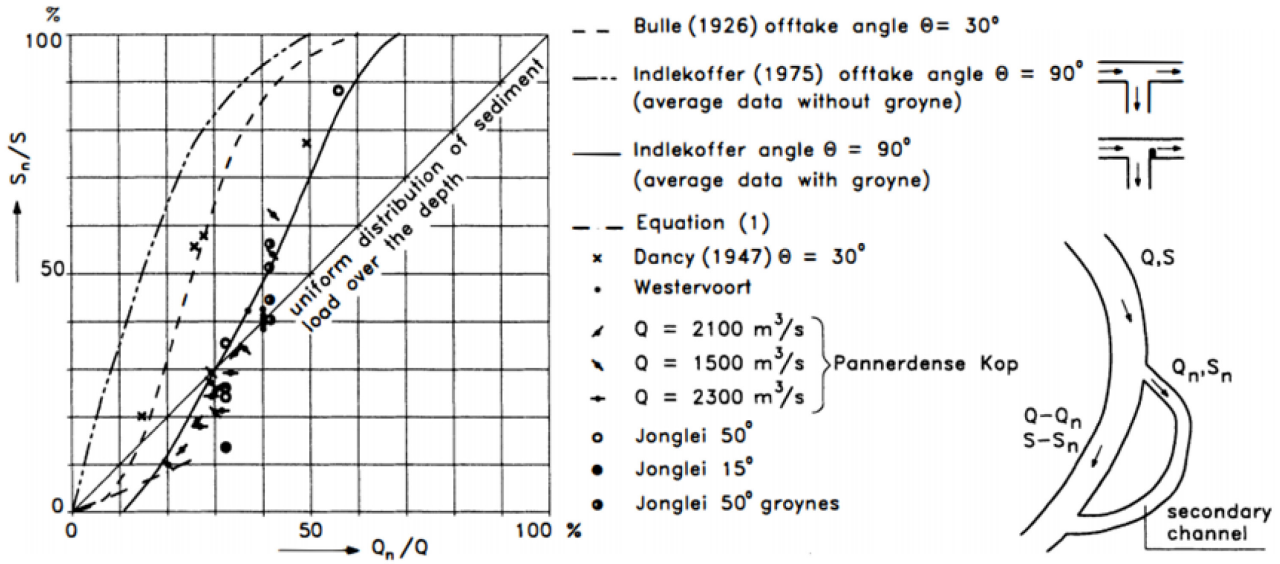

Sediment load in the secondary channel is an influential factor in the instability of the river channel. Since the secondary channel will only carry a small percentage of the main channel discharge, the capacity of the secondary channel to transport sediment is, in general, also much smaller than that of the main channel. In order to avoid the silting up of the secondary channel or periodically dredging, sediment load should be prevented from entering the secondary channel. The following measures can be taken to achieve this goal according to Barneveld et al. (1994):

- The discharge in the secondary channel should be kept small in order to reduce the sediment influx. In general, discharge through the secondary channel should range between 5-10% of the total river discharge (Figure 3).
- Under the low suspended load, the probability of a secondary channel being maintained or abandoned depends mainly on the angle of the off-take. A smaller deflection angle is usually better for the stability of the secondary channel.

2 The study area

The study area is the Wijmeers floodplain of Scheldt River located SE to Schellebelle (Figure 4). The aim of a secondary flood channel construction in this area is to reduce the tide amplitude, as well as the impact of the remaining stagnant water to the adjacent residential area.

The length of Scheldt river in the study area is around 2.8 km, while the min width/depth ratio is about 12 (60 m / 5 m). A cross-section of the river is shown in Figure 5.

Figure 4 – Study area location, Wijmeers in the Upper Sea Scheldt. Cross section of Figure 5 indicated in red

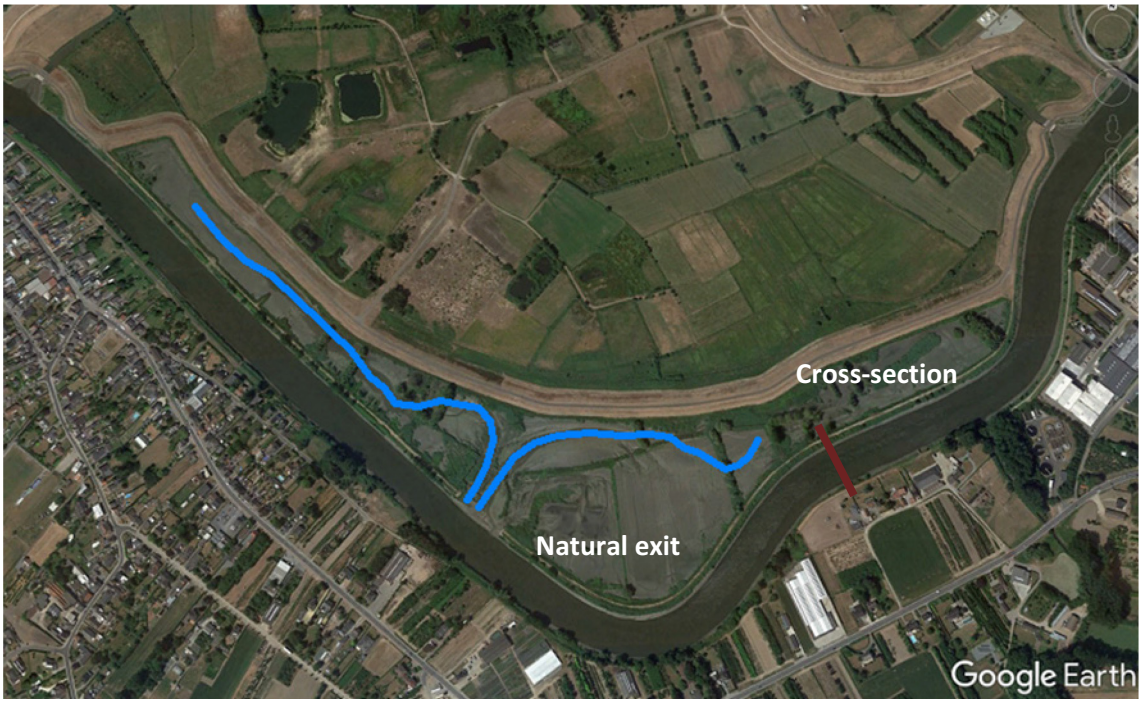

Figure 5 – Cross-section of the main river

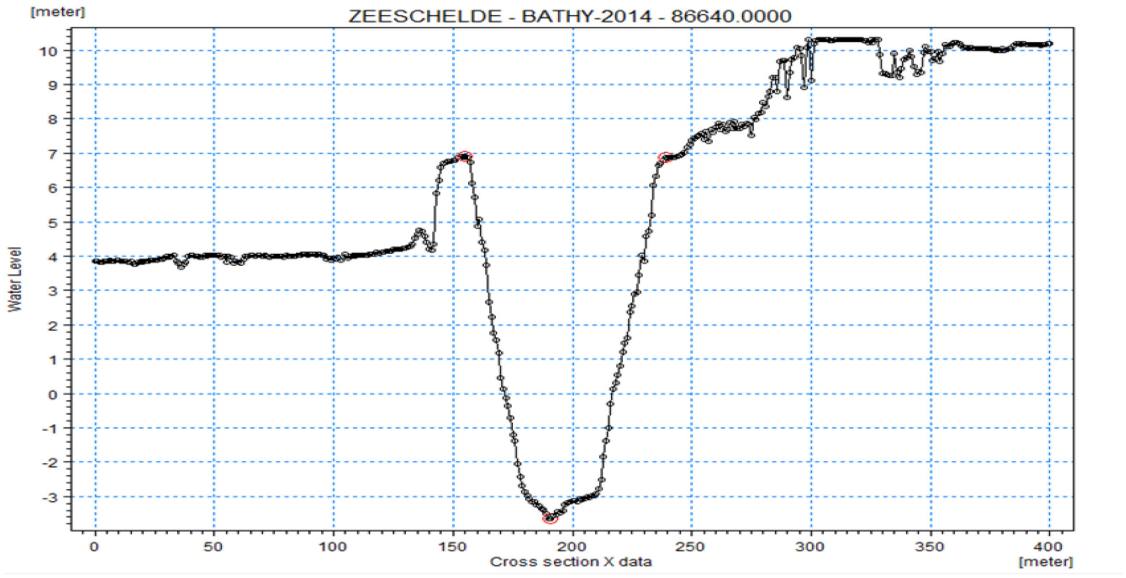

3 Proposed Scenarios

The proposed scenarios are based on the principles from the literature mentioned above and should not deviate much from the natural channel routes that Scheldt river waters seem to follow during the overflow periods at this area.

According to the literature, the ideal off-take angle is less than 30 degrees. Flow velocity should range from 0.10 to 0.80 m/s and width/depth ratio should not deviate much from the width/depth ratio of the main channel. A symmetrical cross-sectional profile corresponding to the natural profile, with steep banks (slope 1:5 to 1:8) could be preferred. As the secondary channel preferably conveys water the whole year round, the deepest section of the secondary channel should be at the most about 2.5 m above the average bed level of the main river, as proposed by Barneveld et al. (1994). Based on the width/depth ratio (60 m / 5 m) of the main river branch, this would mean a max depth of around 2.5 m and a bankfull width of 20-30 m. (IMDC 2019, in prep)

Flood channels have a funneling shape. Towards the upstream end the depth of the channel gradually reduces, and a sill is present at the far end. There is no unique location where the water enters the main or ebb-channel. The can be mimicked by including various bifurcations that branch of and connect to the main river. These branches are less wide and less deep.

The dimensions of the secondary channel can be further improved by investigating the characteristics of the main river, as flow velocity, maximum accepted sedimentation level, bottom slope, width/depth ratio of the main river are important variables of the geometry and the characteristics of the new flood channel.

3.1 The initially proposed scenarios

Initially there were four proposed scenarios for the secondary channel design, named scenario A, B, C and D. No changes are done to the main channel.

3.1.1 Scenario A

The total length of the flood channel in this scenario is around 600 m. The east entrance is designed to be 70m wide. The west outflow (existing) channel is 50 m.

Figure 6 – Scenario A

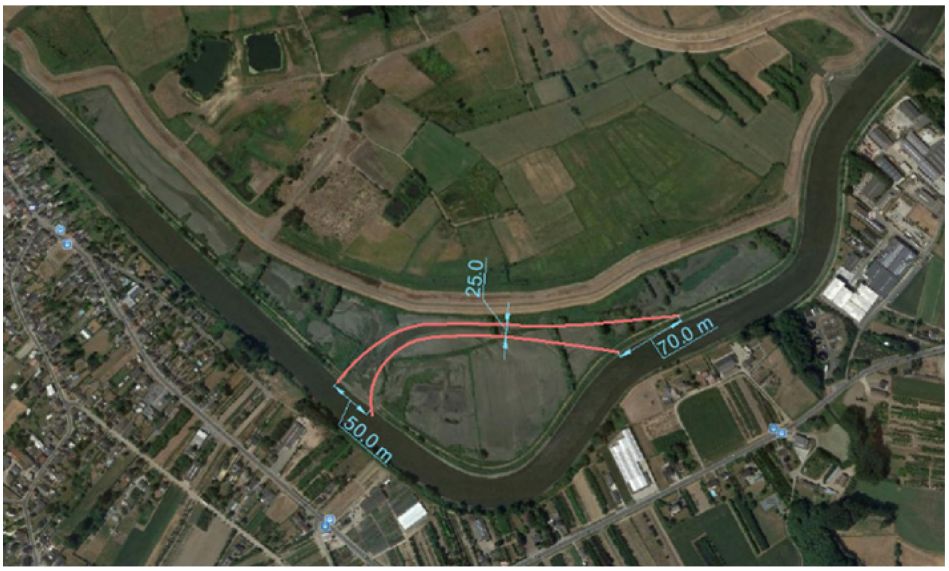

3.1.2 Scenario B

The design of the scenario is similar to Scenario A. In the western part an extra channel is added which ends up in a sill. The total length of the flood channel in this scenario is around 1300 m.

Figure 7 – Scenario B

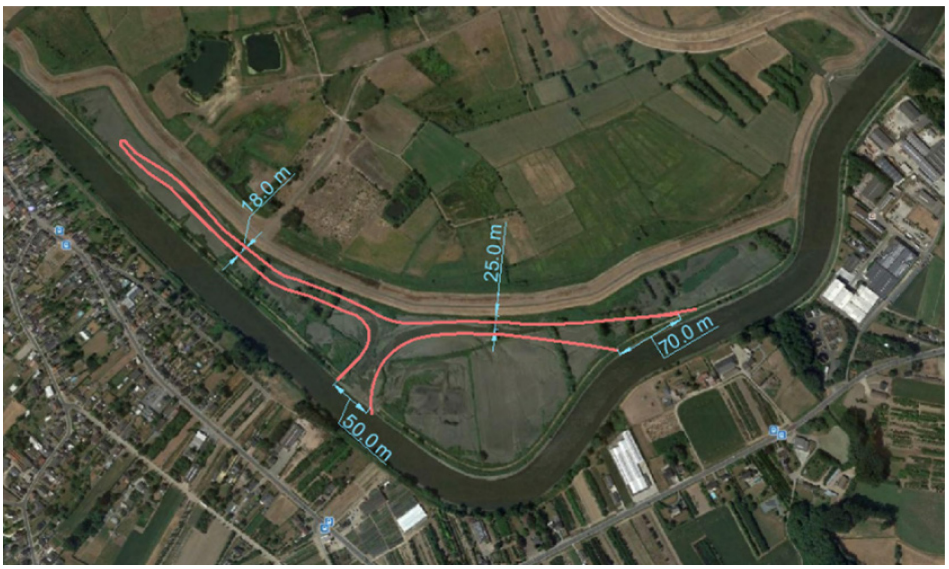

3.1.3 Scenario C

The design of this scenario is similar to Scenario B, but with the inclusion of an extra outflow possibility in the western part. The total length of the flood channel remains around 1300 m. The east branch is wider than the west one.

Figure 8 – Scenario C

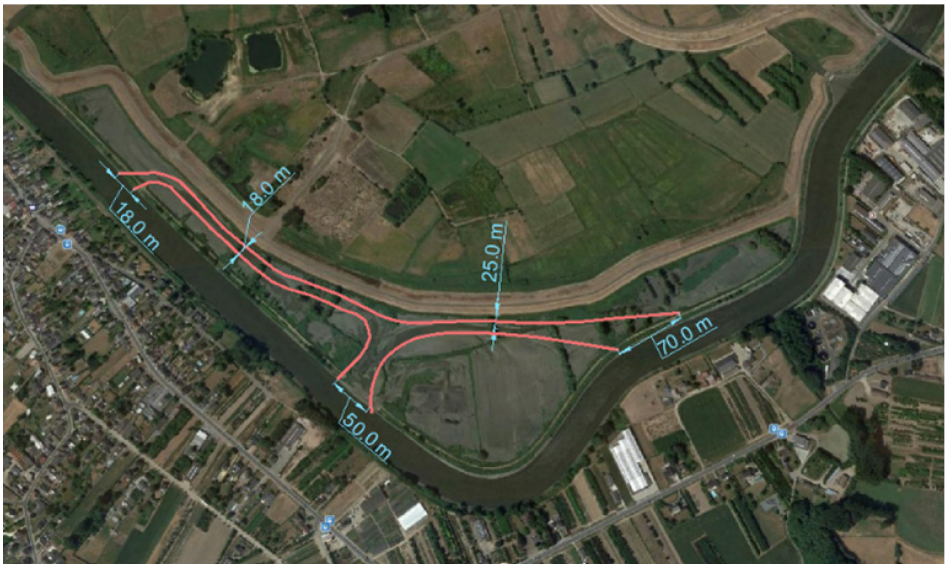

3.1.4 Scenario D

The design of this scenario is similar to Scenario C, but with the inclusion of an extra outflow possibility in the middle part. The total length is around 1400 m.

Figure 9 – Scenario D

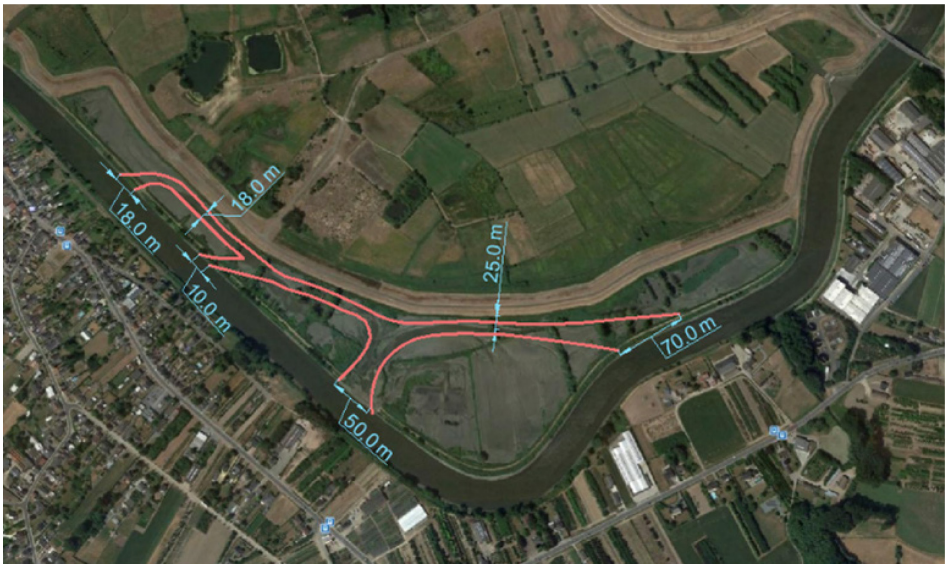

The above scenarios (A, B, C and D) were implemented in the 1D model instrument (MIKE11) and simulations were run to estimate the behavior of each scenario in average conditions. In general, each of the scenarios resulted in (i) a lower maximum high water, (ii) 12% diversion of the discharge and (iii) a low velocity (0.5 m/s) in the flood channel (IMDC, 2019 in prep).

These results should be interpreted with care due the simplified 1D approach. Therefore all results should be further checked with a 2D or 3D model which allows for a more detailed representation and modelling of the flood channel. More in particular the size of the effect on the maximum high water (ca 7 cm) and the flow velocity in the flood channel should be further investigated in detail.

3.2 The newly proposed scenarios

The initial proposed scenarios (A, B, C and D) were discussed amongst a technical working group on 13th February 2019. No clear benefit was detected in scenario B and D and therefore these are not considered further.

The technical working group suggested four scenarios to be studied more in detail using a 2D approach. The rationale between the definition of the scenarios is to get a clear view of the effect of (i) the length of the flood channel and (ii) inlet and outlet levels of the flood channel. A summary of the reference and the scenarios is presented in Table 1.

Table 1 – Scenarios

	Inlet level (mTAW)	**Downstream outflow (mTAW)**	**Upstream outflow (mTAW)**
Reference	as is	as is	as is
Scenario A	2	2	as is
Scenario E1	2	as is	2
Scenario E2	2.5	as is	2.5
Scenario E3	2.5	as is	3

“as is” indicates that no changes are made with respect to the current situation.
This means that there is no explicit connection between the Scheldt and the flood plain at this location

Figure 10 – The current situation, and design plans of scenario A (red) and the three E-variants (blue)

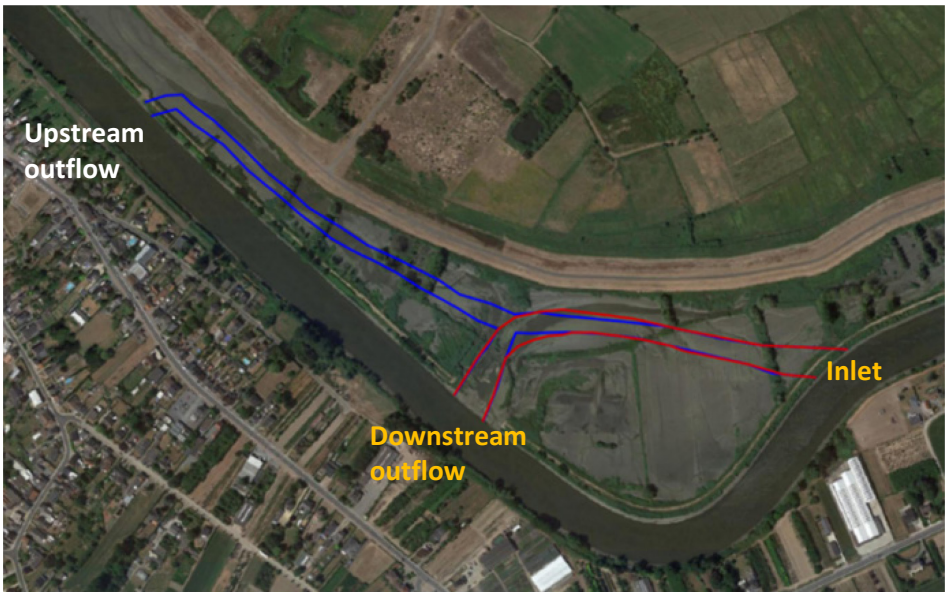

A first scenario is a duplicate of the scenario presented in this report as scenario A and is the 'short' variant. The other three suggested scenarios (scenario E1, E2 and E3) are 'long' variants of the flood channel. These scenarios have an additional outlet located more upstream when compared to Scenario A. The three E-variants have the same outline of the secondary channel (Figure 10), but different bottom elevations in the inlet and the outflows, as listed in Table 1.

The implemented bathymetries A-E3 are visualized in the next section in Figure 13 to Figure 16.

4 Modelling Hydrodynamics

A 3D model is made to simulate the hydrodynamics in different scenarios. This model has a relatively small scale, with a focus on the study area. It is based on the SCALDIS model, which is developed with TELEMAC-3D and calibrated for the Scheldt estuary (Smolders et al. 2016).

4.1 The Mathematical Model

The hydrodynamics is modelled with 3D incompressible Reynolds-averaged Navier-Stokes equations in TELEMAC-3D. Assuming that fluid density is constant, and applying the Boussinesq approximation to the Reynolds stress term, the mass and momentum conservation equations read:

$$\nabla \cdot \boldsymbol{u} = 0 \tag{1}$$

$$\frac{\partial \boldsymbol{u}}{\partial t} + (\boldsymbol{u} \cdot \nabla)\boldsymbol{u} = -\frac{1}{\rho}\nabla p + \nabla \cdot [(\nu + \nu_T)\nabla \boldsymbol{u}] + \boldsymbol{g} + \boldsymbol{F} \tag{2}$$

where $\boldsymbol{u}$ is the Reynolds-averaged mean velocity field, t is the time, ρ is the fluid density, p is the mean pressure, ν is the kinematic viscosity of the fluid, ν_T is the turbulence eddy viscosity, $\boldsymbol{g}$ is the gravitational force and $\boldsymbol{F}$ is the other external forces, e.g. Coriolis force and centrifugal force.

In many industrial and environmental flows, the density of the carrying phase is not a constant but varies as a function of the temperature, salinity and/or sediment concentration. The buoyancy effects due to the density gradient thus should be included in the governing equations in order to model the stratifications properly. The varying density could be included in the equation (1) and (2). But there is also an alternative way that enables the treatment of buoyancy effect by means of the gravity term if the change of density $\Delta\rho/\rho < 0.1$. Based on this assumption, an extra term representing the buoyancy force can be derived and added into the equation (2).

To solve the above equations, a turbulence model should be provided as the closure for ν_T. In the large-scale modelling, the water depth is often not in the same order of magnitude comparing to the horizontal dimensions of the domain. Hence, the domain discretization usually leads to a much coarser mesh resolution in horizontal, and relatively finer mesh resolution in vertical, meaning that the turbulence eddies that represented in horizontal and in vertical are of different scales. Hence, in this study, two turbulence models are employed. The Smagorinski model is used for modelling the horizontal turbulent eddy viscosity. Smagorinski's idea is to add to the molecular viscosity a turbulent viscosity deduced from a mixing length model. This mixing length corresponds to the size of the vortices smaller than that of the mesh size. In this way, it is able to compensate the turbulence diffusion with smaller vortices that is inhibited by the mesh and the computational cost is lower than the two-equation turbulence models. The Smagorinski model has the form:

$$\nu_T = C_s^2 \Delta^2 \sqrt{2\boldsymbol{S}:\boldsymbol{S}} \tag{3}$$

where C_s is dimensionless coefficient to be calibrated, Δ the mesh size derived from the volume of the elements in 3D, and $\boldsymbol{S}$ is the mean rate-of-strain tensor.

The mixing-length model, including turbulence damping, is applied for solving the vertical eddy viscosity. This is also a relatively simple approach, which is based on the assumption that turbulent eddies, like gas molecules, are discrete entities that collide and exchange momentum at discrete intervals, so called the characteristic length or mixing length. Then a relationship between eddy viscosity and mixing length,

including a damping function, can be established as:

$$\nu_T = L_m^2 \sqrt{2\boldsymbol{S}:\boldsymbol{S}} \tag{4}$$

where L_m is the mixing length and its formula is given in many studies with different forms. In the current study, Nezu & Nakagawa model for determining the mixing length is used:

$$L_m = \kappa z \sqrt{1 - \frac{z}{h}} \tag{5}$$

where κ is the von Karman constant, z is the distance to the bed, h is the water depth.

4.2 Model Setup

4.2.1 Mesh and bathymetry

In order to be more efficient for assessing the scenarios and alternatives with more details, the 3D hydrodynamic model adopts a much smaller domain comparing to that of the SCALDIS model, only focusing on the study area.

The domain is cut off from the SCALDIS model, extending about 2 - 2.5 km towards both upstream and downstream from Wijmeers (Figure 11). The mesh is then refined to a resolution of about 4m in the area of interest, which is sufficient to capture the secondary channels and local topographical features.

The mesh has 51861 nodes and 100428 elements in one horizontal plane. In the 3D model, the domain is discretized into 6 horizontal planes, distributed uniformly over the vertical. This is one more vertical interface than in the original Scaldis model. The smaller model can have more vertical resolution and still run efficiently.

Figure 11 – The mesh and bathymetry of the 3D hydrodynamic model

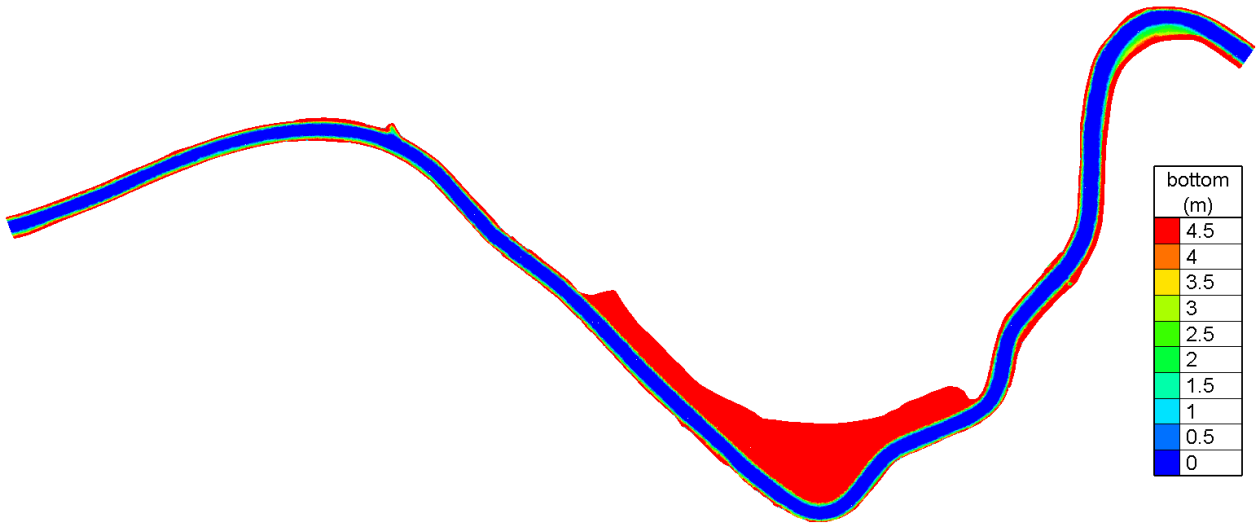

The bathymetry is taken from a Digital terrain model (DTM), derived from aerial surveys. The DTM contains the natural situation of the domain. The bathymetry data of the four scenarios was provided by De Vlaamse Waterweg nv. Four bathymetry files were provided, corresponding to the scenarios A, E1, E2 and E3 (Figure 13 - Figure 16).

Figure 12 – Bathymetry for the reference (current situation)

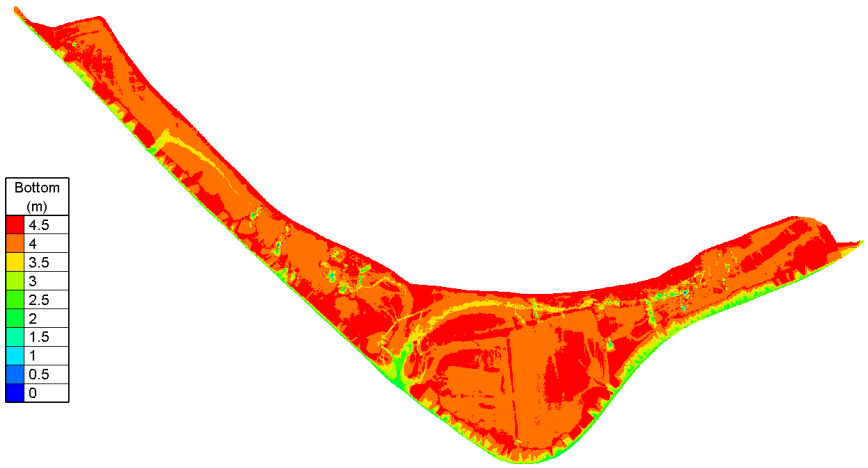

Figure 13 – Bathymetry for scenario A

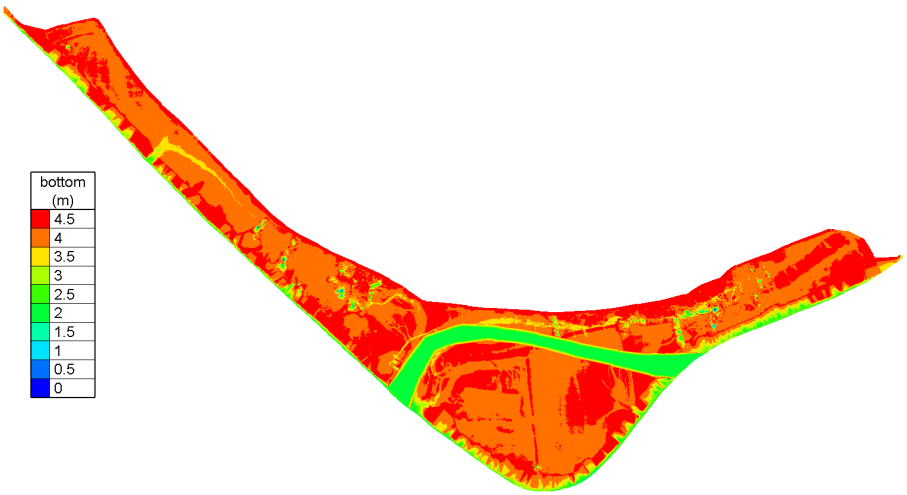

Figure 14 – Bathymetry for scenario E1

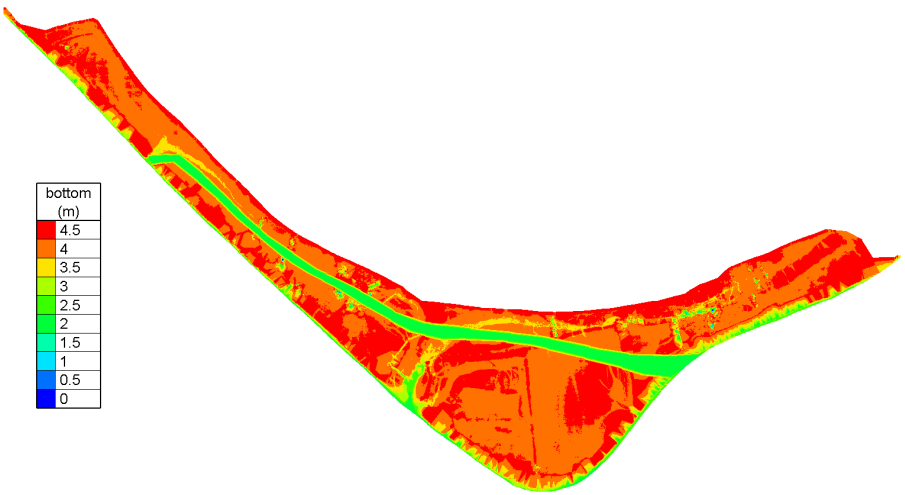

Figure 15 – Bathymetry for scenario E2

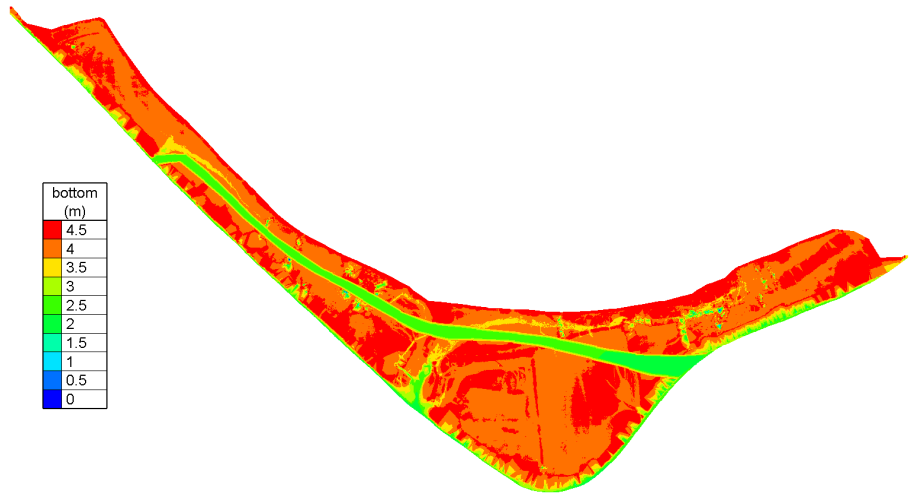

Figure 16 – The bathymetry of the scenario E3

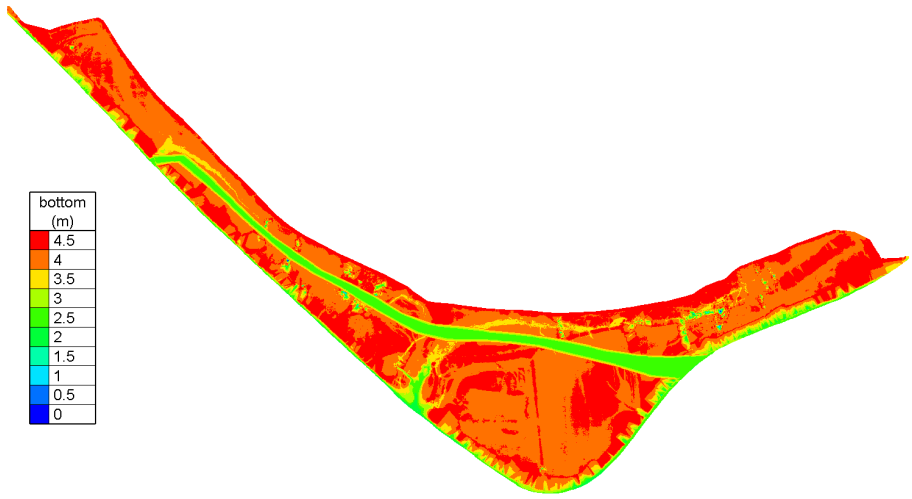

The bottom elevation along the secondary channel, is given in Table 1 for the end points, and is plotted below along the thalweg (Figure 17 - Figure 20).

Figure 17 – The points along the thalweg of the secondary channel in the scenario A

Figure 18 – Bottom elevation [mTAW] in the secondary channel (scenario A)

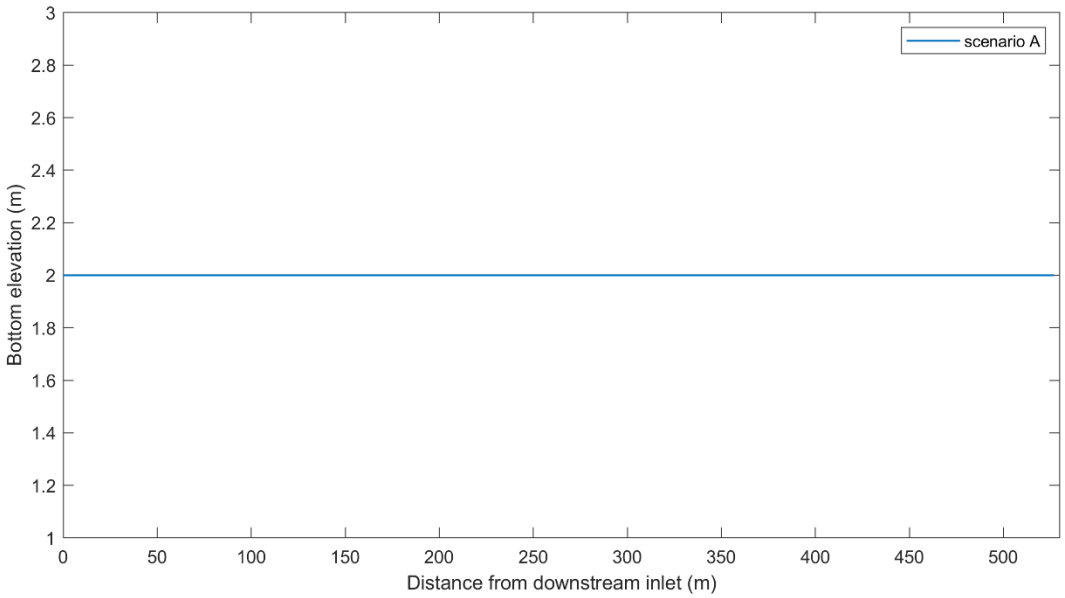

Figure 19 – The points along the thalweg of the secondary channel in the scenario E

Figure 20 – Bottom elevation [mTAW] in the secondary channel (scenario E)

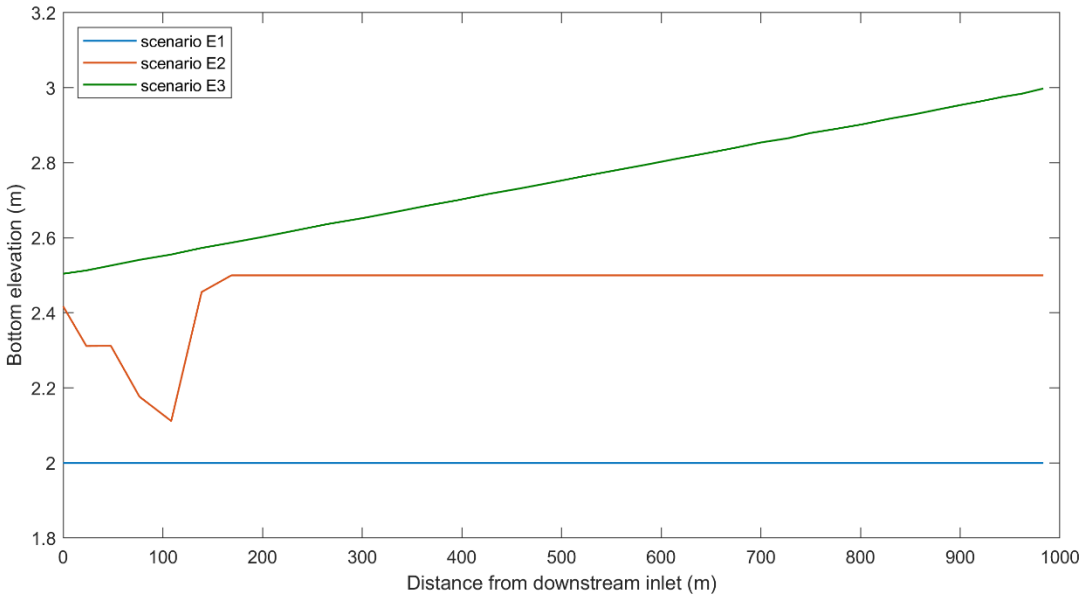

Five model grids are made by mapping different bathymetry data of the area Wijmeers onto the mesh, one for the reference situation, the other four are for the scenarios A, E1, E2 and E3.

4.2.2 Boundary conditions

There are two open boundaries defined in the hydrodynamic model, one at downstream and the other one at upstream (Figure 21). In both of them, time series of flow rate are imposed.

Figure 21 – Open Boundaries defined in the model (green – downstream boundary, blue – upstream boundary)

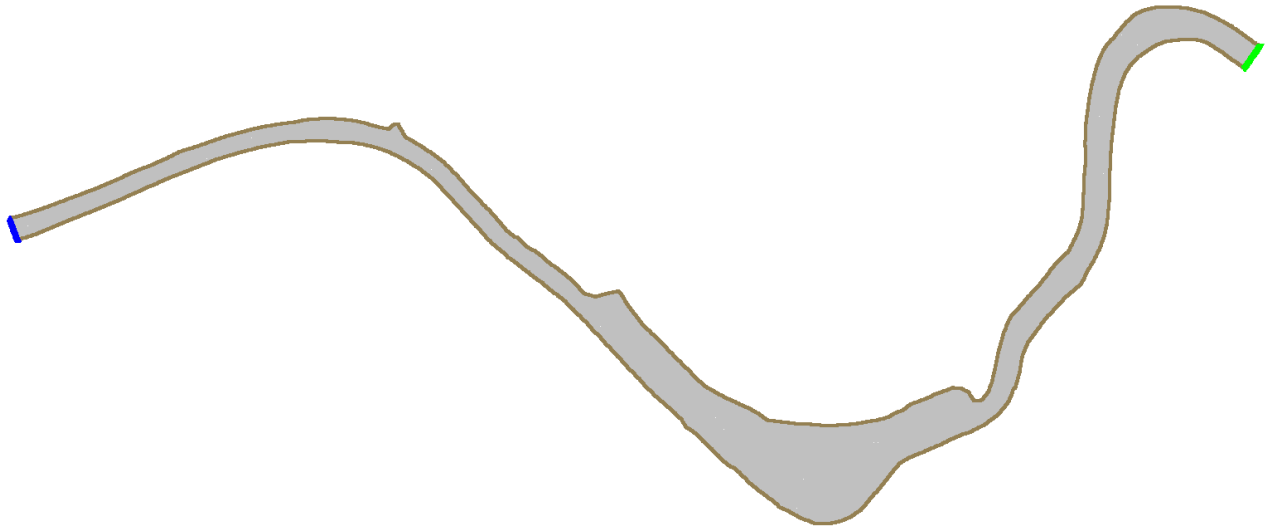

The boundary conditions are calculated in the SCALDIS model for the period from 31/07/2013 22:20:00 to 09/09/2013 22:20:00 (Figure 22).

Figure 22 – Downstream and upstream boundary conditions

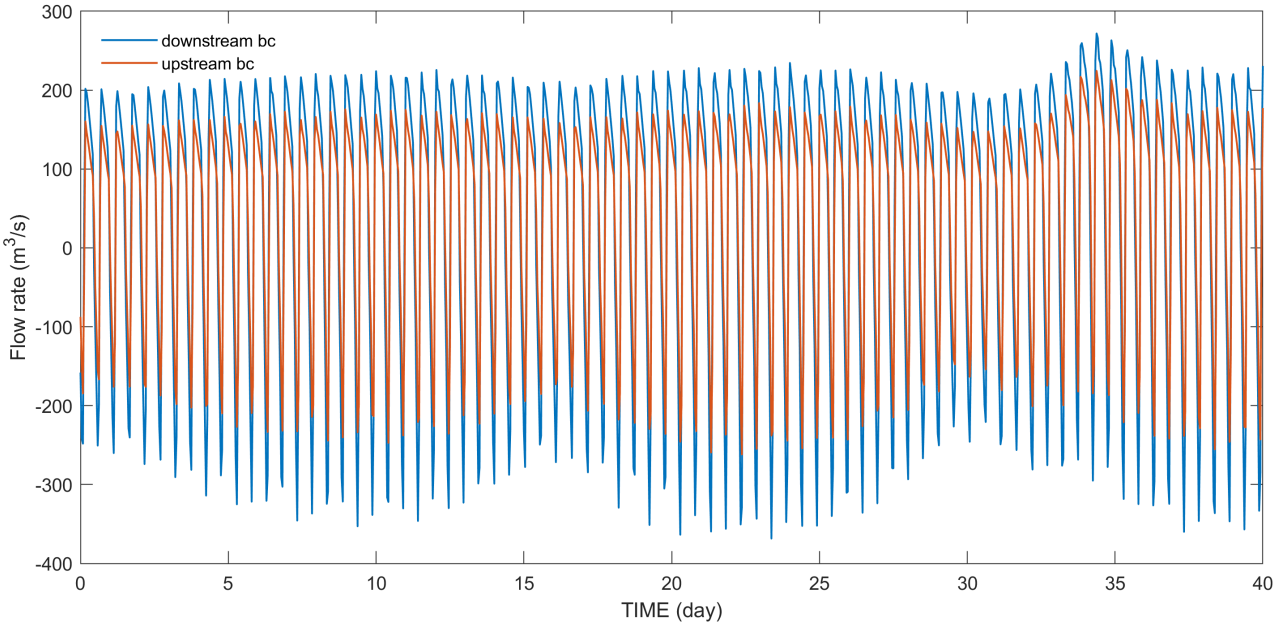

4.2.3 Initial conditions

The model is initialized with a constant elevation of 3.20 m, and zero velocity across the entire domain.

4.2.4 Other model settings

The manning coefficient is used as the bottom roughness. In the current study, a constant value of 0.02 is used. The treatment of tidal flat is enabled in the model, in order to properly model the drying and wetting in each tidal cycle.

4.3 Validation

As validation, the detailed model for Wijmeers has been compared at several locations with the original SCALDIS model in terms of water level and velocity components.

In the SCALDIS model, the floodplain is behind the dike and there is no overflow during the simulation period. For fair comparison, the same bathymetry from the SCALDIS model is used in the Wijmeers model for the validation.

It is worth mentioning that the smaller scale Wijmeers model has finer resolution of the grid, one more horizontal plane in vertical for better accuracy, and shorter time interval for output of the results (10min instead of 60min), therefore, it is expected to have slight differences in the comparisons.

Figure 23 – The bathymetry used for validation and the comparisons with the SCALDIS model at four locations

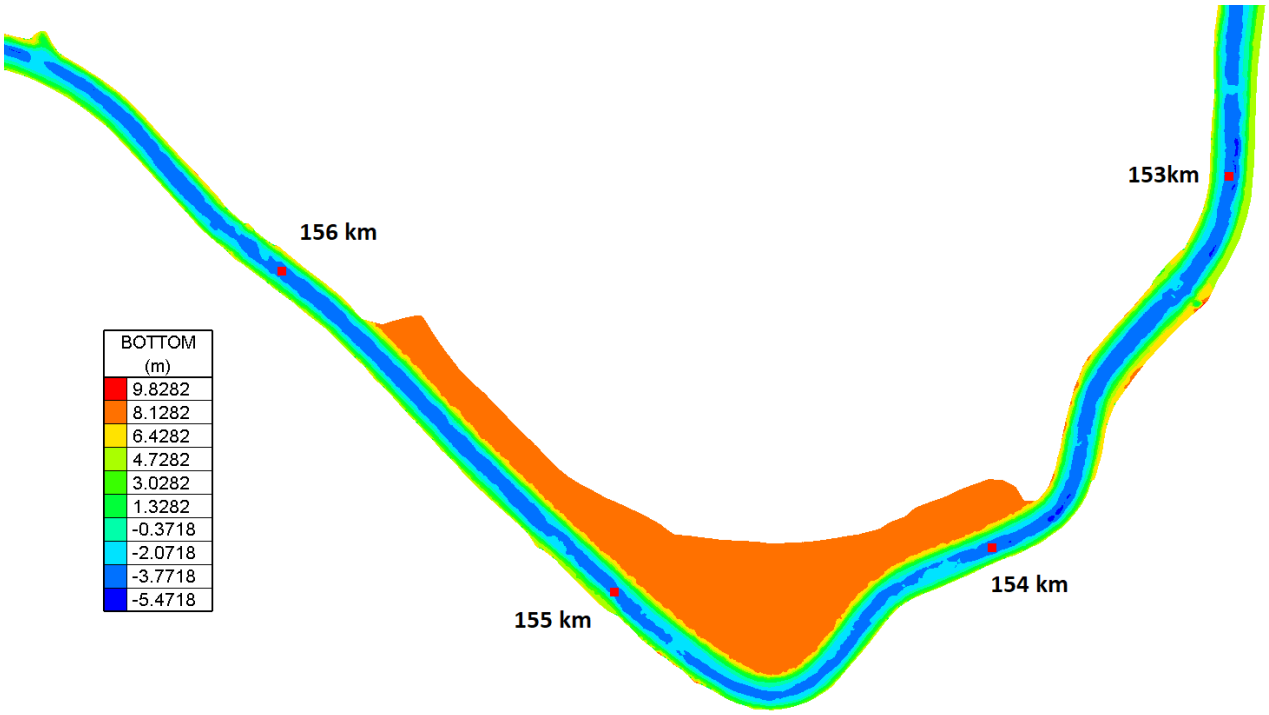

The water levels at these four locations are compared and shown in the figures below. It can be seen that the water levels in the smaller scale model for Wijmeers has a good agreement with the results from the original SCALDIS model, where its boundary conditions are extracted.

For the comparison of velocity magnitude, in general the results from the Wijmeers model matches well with the results from the SCALDIS model. But due to the shorter time interval of the output, the Wijmeers model gives lower velocity during the slack tide, meaning that it captures more details during the transition period. There are slight differences at the locations 155km and 156km during certain moments in the ebb phase, but the differences are less than 2.5%.

Figure 24 – Water level comparison at 153 km from Vlissingen

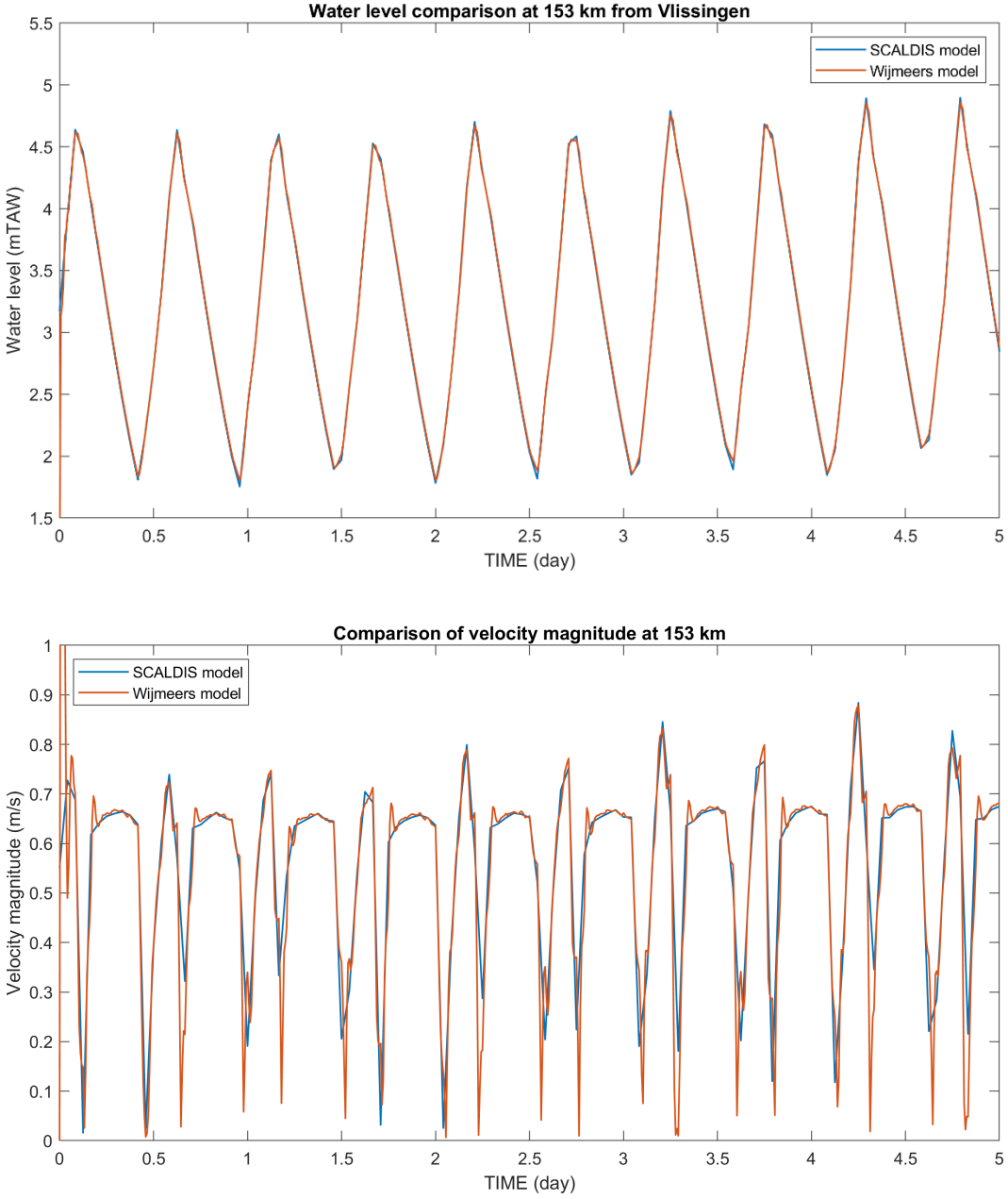

Figure 25 – Water level comparison at 154 km from Vlissingen

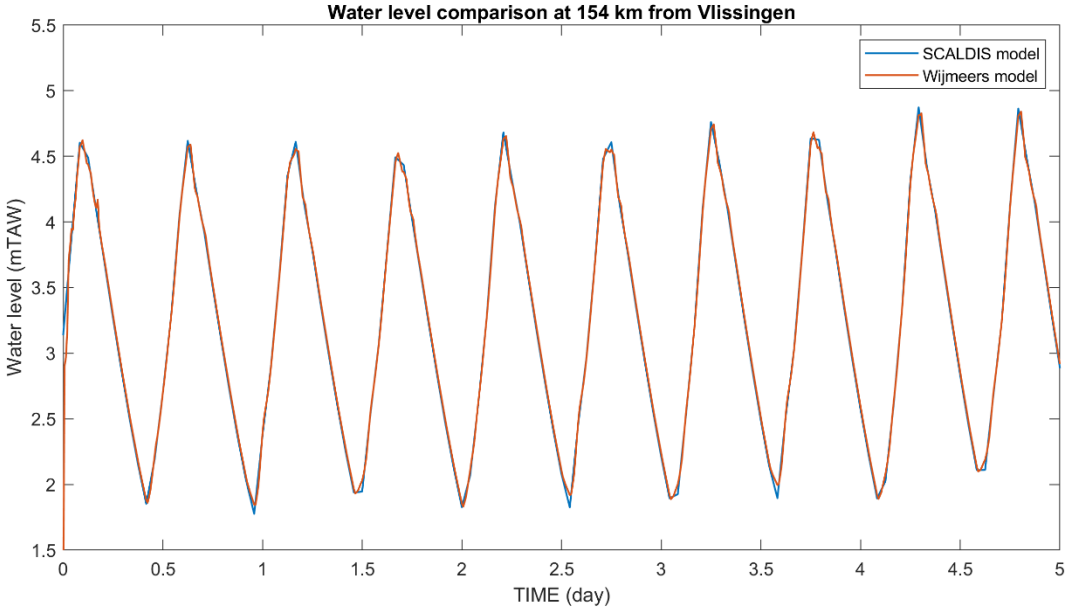

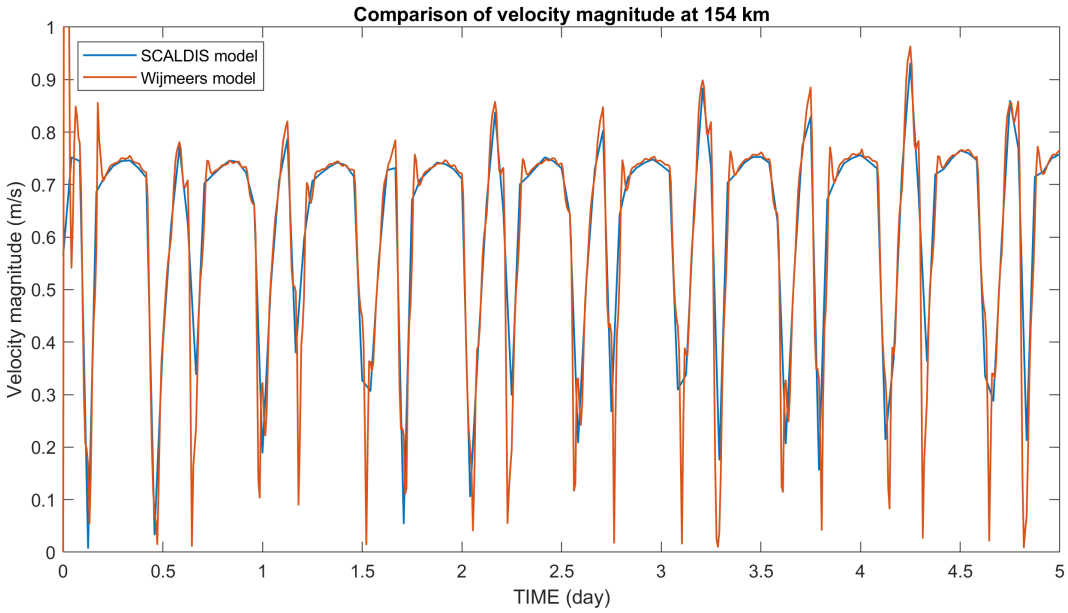

Figure 26 – Water level comparison at 155 km from Vlissingen

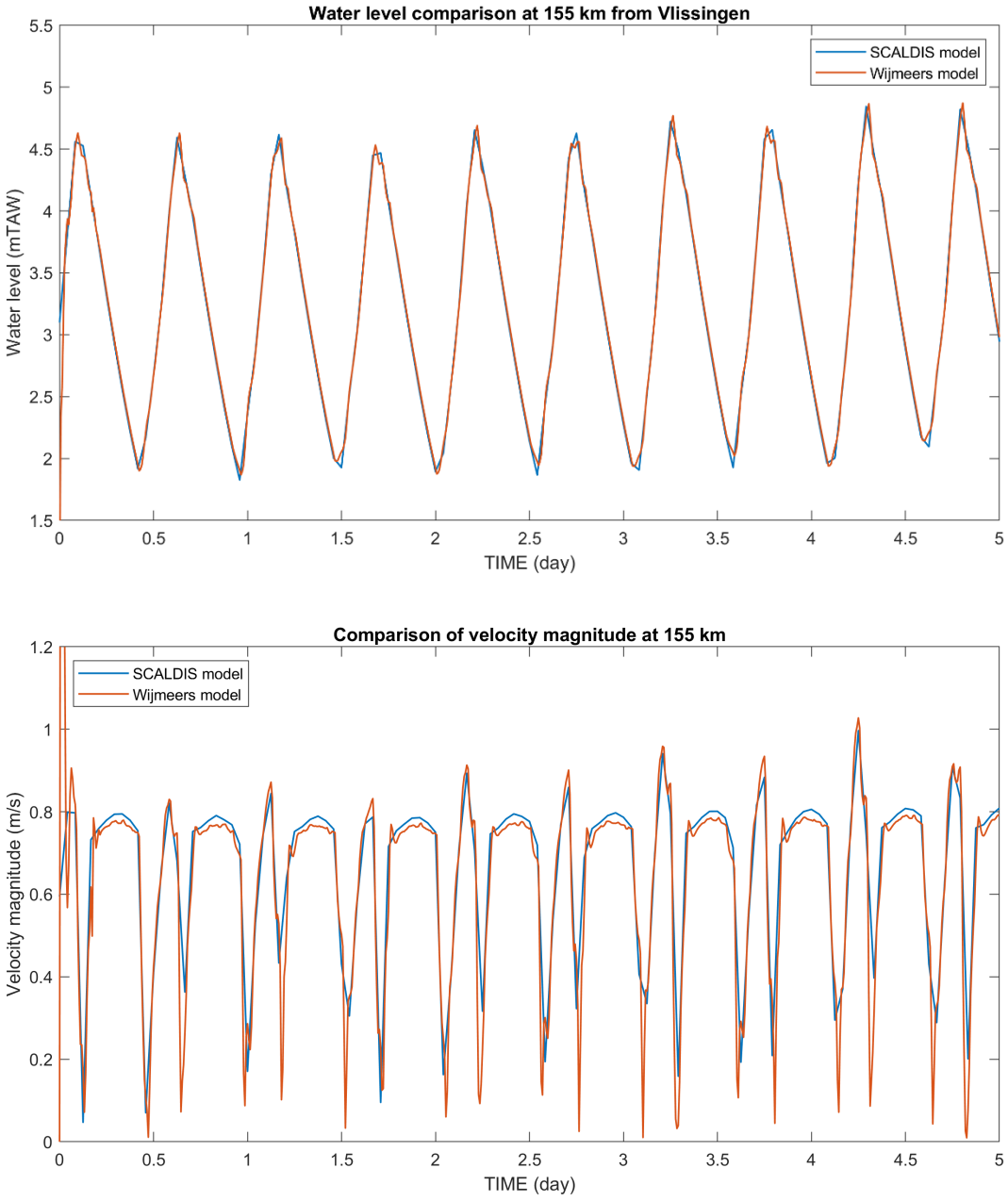

Figure 27 – Water level comparison at 156 km from Vlissingen

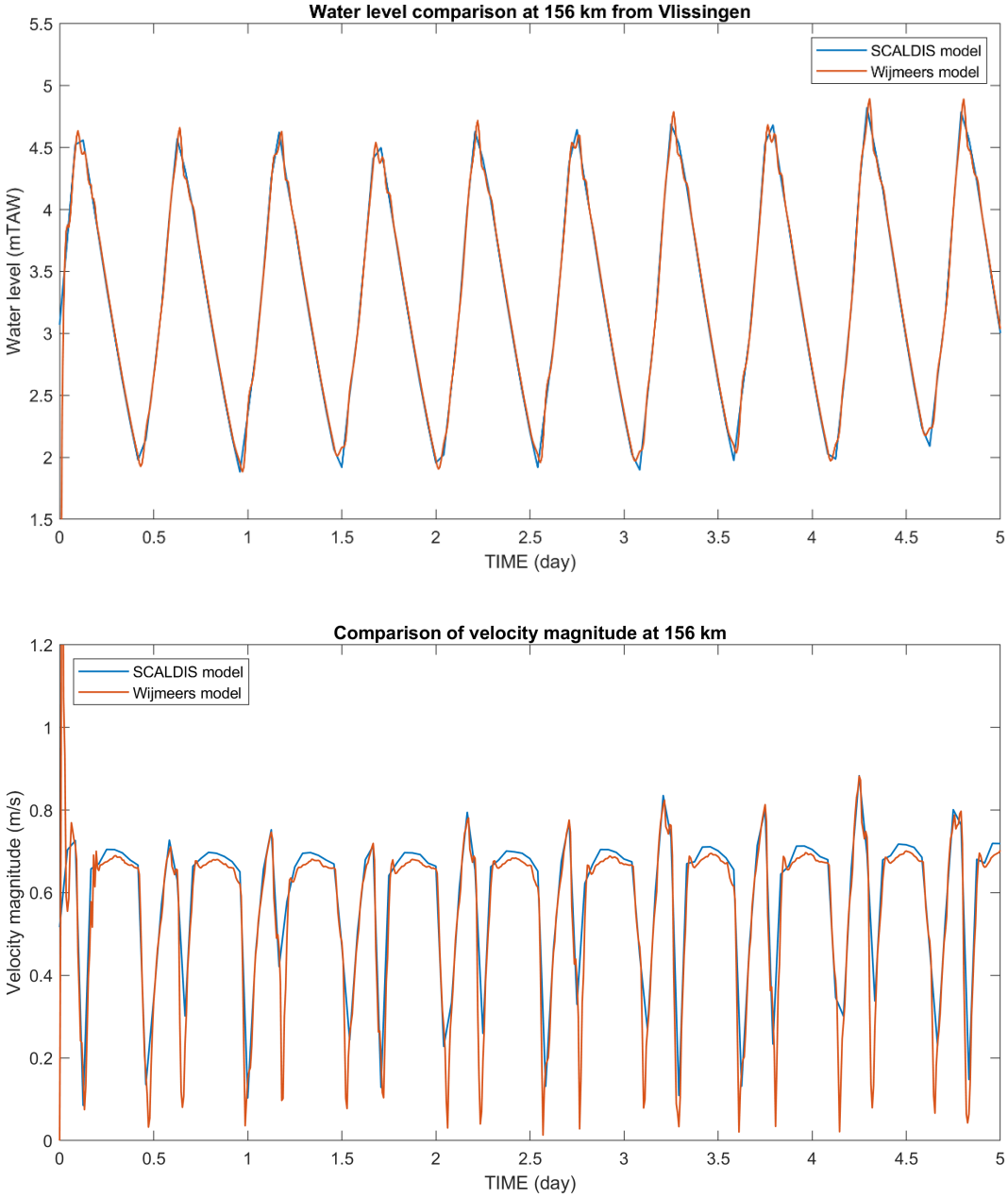

Based on the above comparison, we could come to the conclusion that the smaller scale Wijmeers model performs as well as the original SCALDIS model in terms of predicting flow field in the simulation period.

5 Results

5.1 Discharge

The discharges calculated from the model results in secondary channel and the main channel are analyzed. There are 7 transects defined in the domain, in order to have a clear view about how the flow is distributed between the main flow path and the diversions.

Figure 28 – The transects defined in the domain

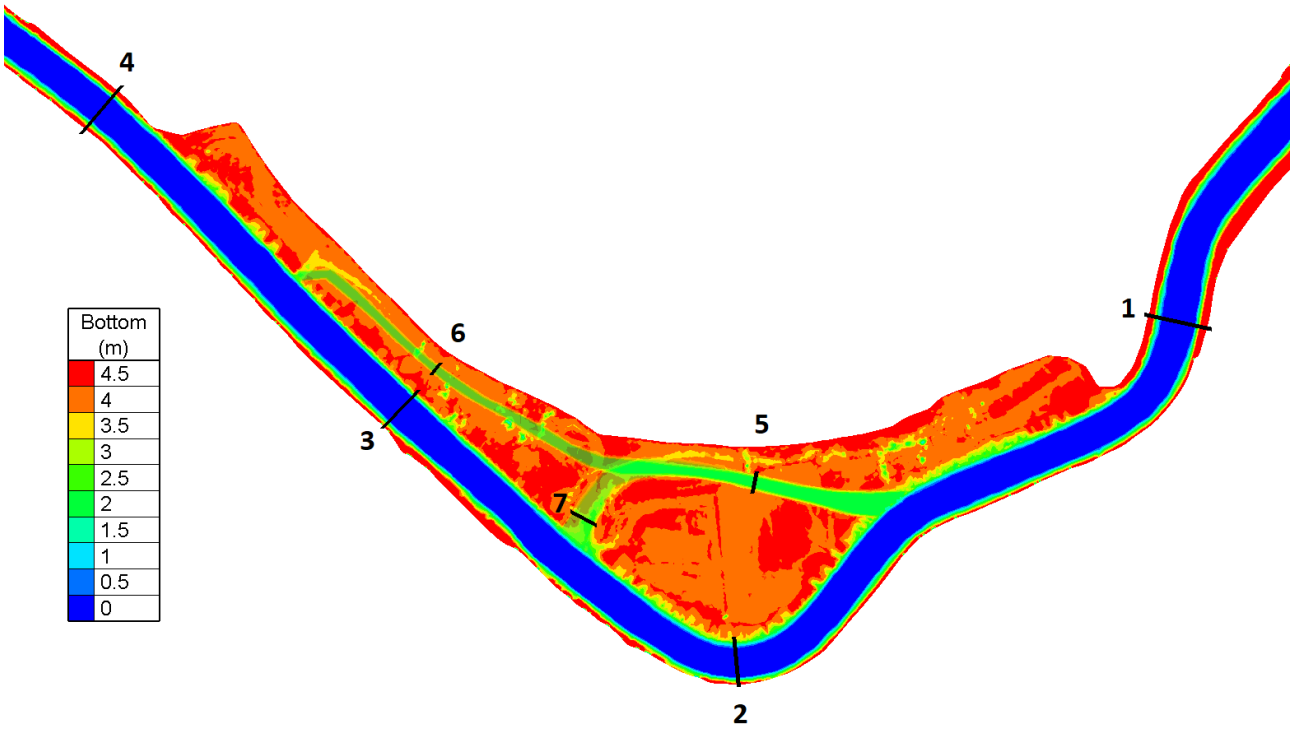

The time series of discharges at all the 7 transects are computed from the model results and plotted for each scenario (Figure 29 - Figure 32). Here we only show one transect in the main channel since the differences are in general small. Positive (negative) values mean the discharge is directed downstream (upstream).

Figure 29 – Discharges at transect 2 for all the scenarios.
Positive (negative) values mean the discharge is directed downstream (upstream)

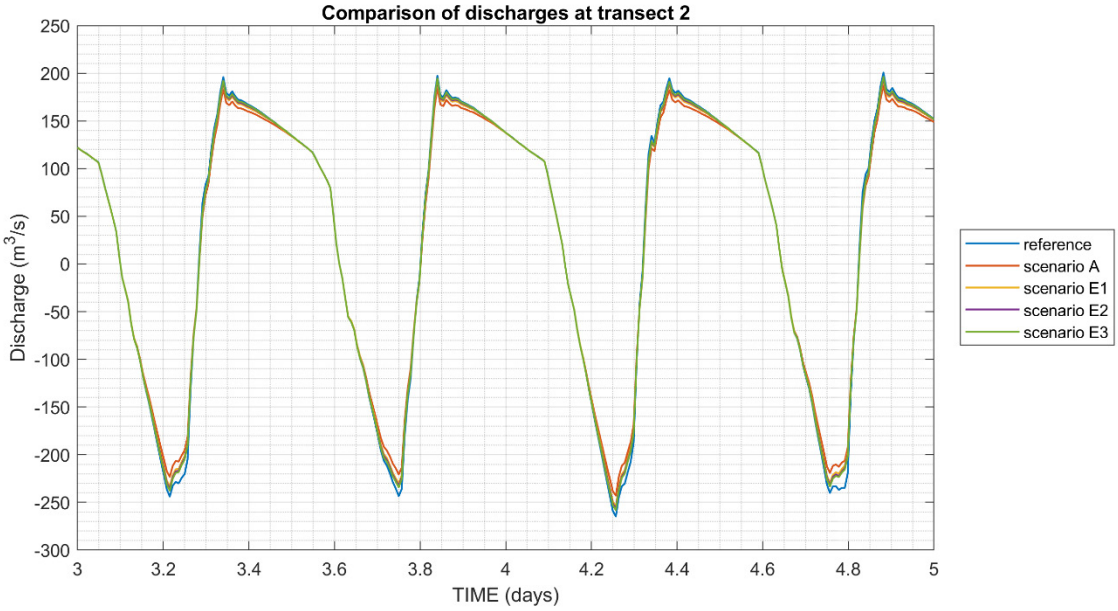

Figure 30 – Discharges at transect 5 for all the scenarios.
Positive (negative) values mean the discharge is directed downstream (upstream)

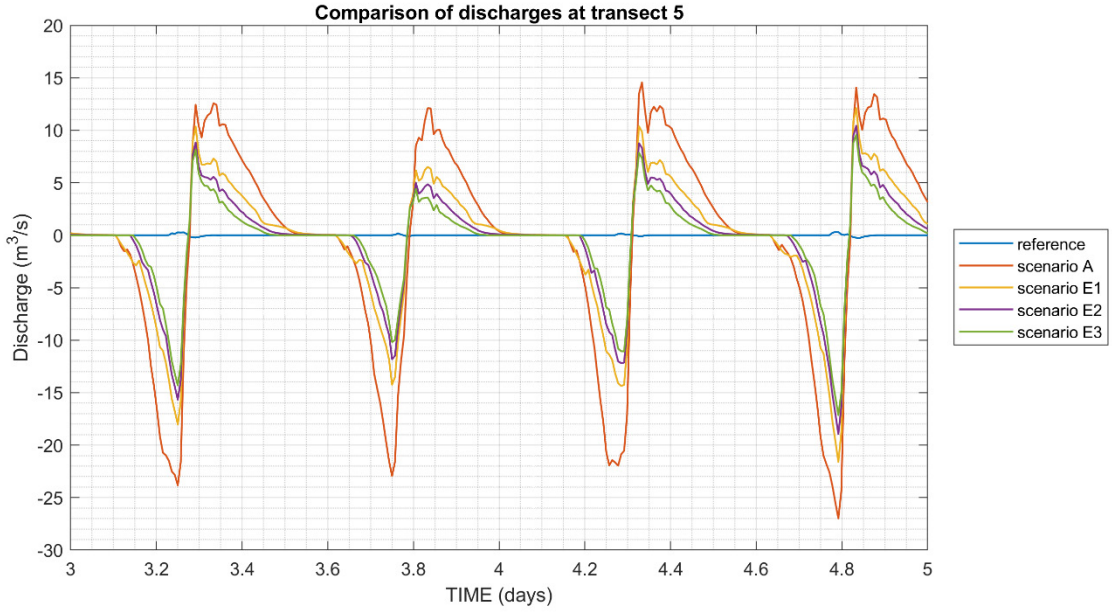

Figure 31 – Discharges at transect 6 for all the scenarios.
Positive (negative) values mean the discharge is directed downstream (upstream)

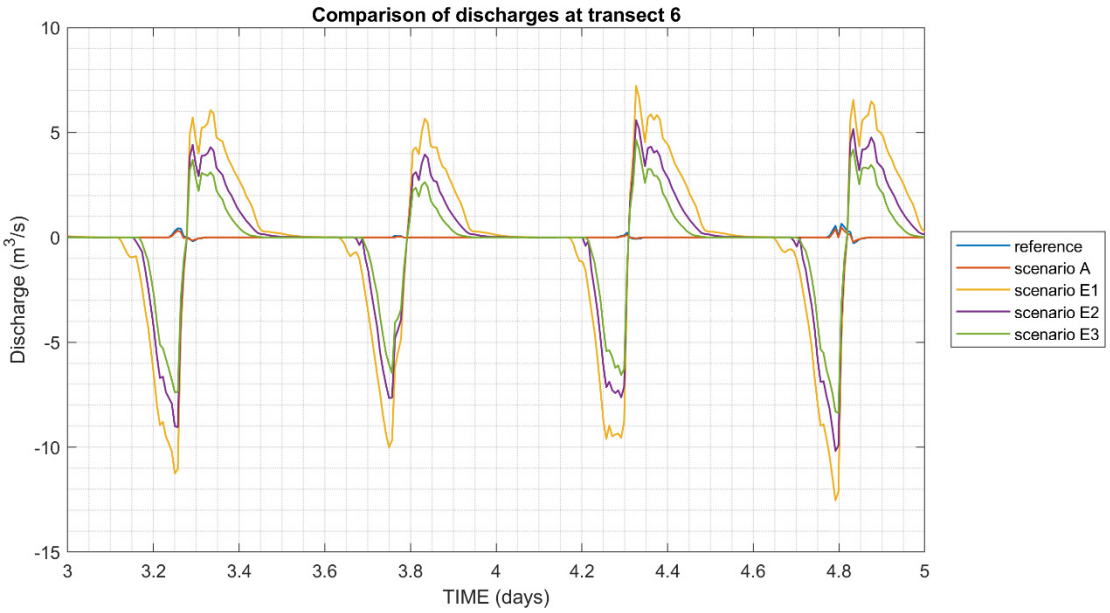

Figure 32 – Discharges at transect 7 for all the scenarios.
Positive (negative) values mean the discharge is directed downstream (upstream)

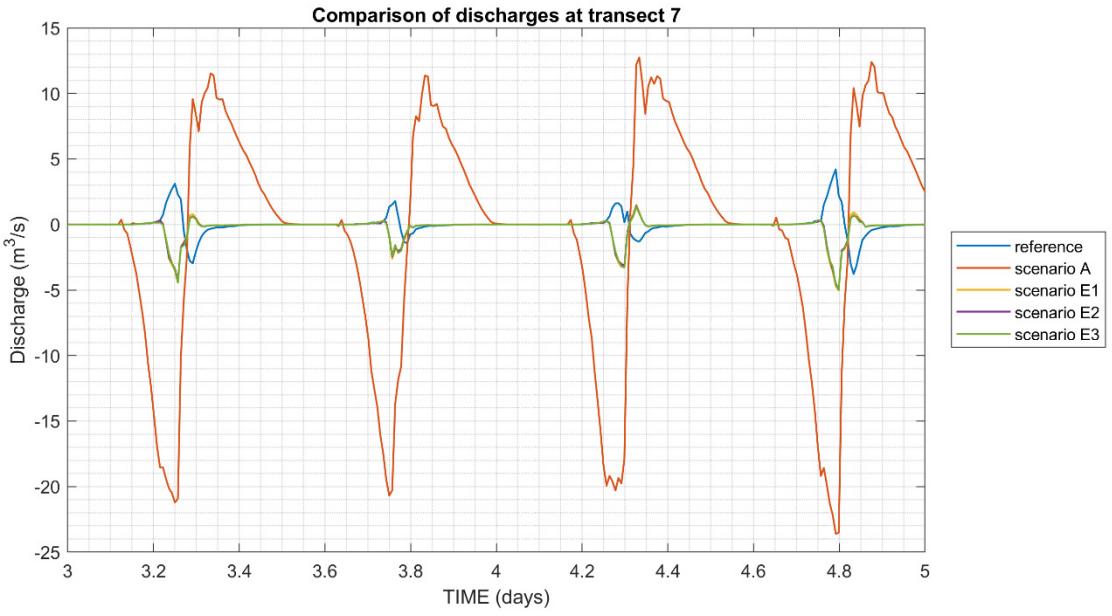

Maximum discharges during ebb and flood tide are calculated for each transect and for each scenario. They are expressed as a ratio to the maximum discharge in transect 1 (Table 2 and Table 3).

Table 2 – The percentage (%) of discharges at transects comparing to the total discharge (ebb tide)

	Transect 1	Transect 2	Transect 3	Transect 4	Transect 5	Transect 6	Transect 7
Reference	100.00	97.05	94.05	90.51	0.15	0.31	2.04
Scenarios A	100.00	90.35	93.48	90.08	7.03	0.23	6.15
Scenarios E1	100.00	93.30	90.59	89.97	5.85	3.49	0.73
Scenarios E2	100.00	94.21	91.47	90.00	5.04	2.70	0.68
Scenarios E3	100.00	94.83	92.11	90.01	4.62	2.25	0.65

Figure 33 – The percentage (%) of discharges at transects comparing to the total discharge (ebb tide)

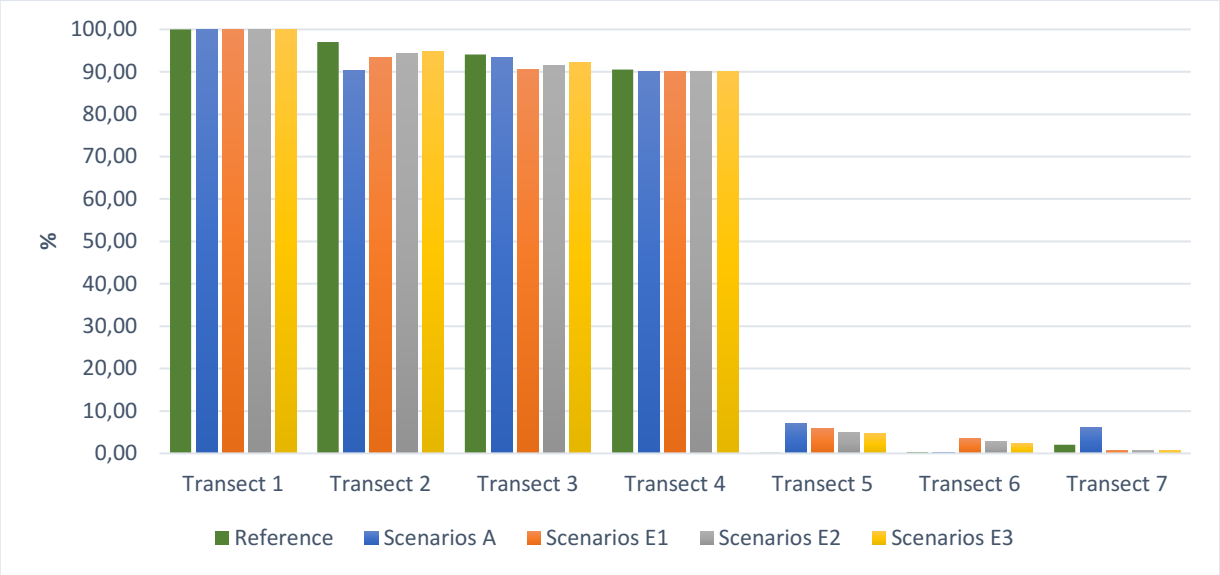

Table 3 – The percentage (%) of discharges at transects comparing to the total discharge (flood tide)

	Transect 1	Transect 2	Transect 3	Transect 4	Transect 5	Transect 6	Transect 7
Reference	100.00	95.97	92.39	88.44	0.10	0.10	1.37
Scenarios A	100.00	87.77	91.68	87.94	9.76	0.09	8.53
Scenarios E1	100.00	91.67	88.00	87.51	7.79	4.52	1.82
Scenarios E2	100.00	92.50	89.02	87.53	6.84	3.67	1.80
Scenarios E3	100.00	93.10	89.69	87.55	6.19	3.02	1.80

Figure 34 – The percentage (%) of discharges at transects comparing to the total discharge (flood tide)

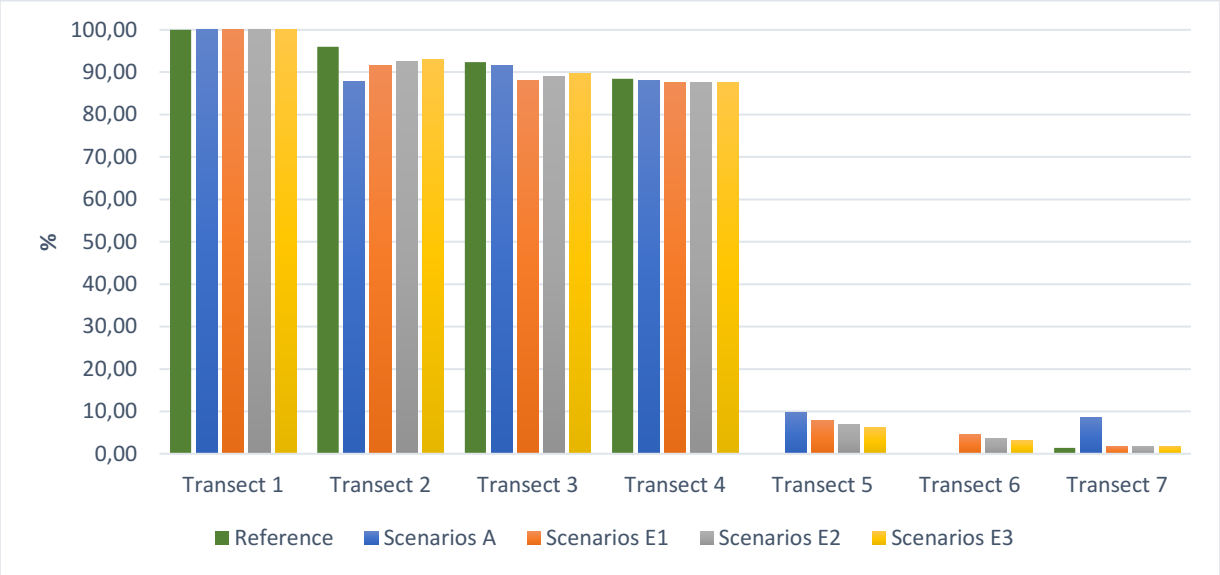

The Wijmeers floodplain lies below high water level so at high water level there is overflow, which complicates the interpretation of the discharges. But it is clear that scenario A has the highest discharge in the secondary channel comparing to the E-variants. Among all the E-variants, E1 has the largest discharge in the secondary channel.

5.2 Inundation frequency

The inundation frequency is an important index for evaluating the ecological influence on the floodplain, especially for the floodplain vegetation. In this report, the inundation frequency is computed from the model results according to the definition:

$$f_{inundation}(x,y) = \frac{T_{wet}(x,y)}{T_{total}(x,y)} \quad (1)$$

in which, T_{wet} is the duration of the point being wet in the domain, T_{total} is the period of a spring-neap cycle, (x,y) represents the location of each point in the domain.

The inundation frequency map is generated based on the above formula and shown in the figures below.

As seen from the figures, the inundation frequency is generally small on the floodplain, except in the secondary channel and at some locations, where the bottom elevation is lower than the neighboring area and water is always presented.

The other thing that can be noticed is that the inundation frequency decreases when the bottom elevation increases in the E scenarios. The most noticeable effects is from scenario E3, in which the inundation frequency decreases in the secondary channel.

Figure 35 - Inundation frequency of the reference case

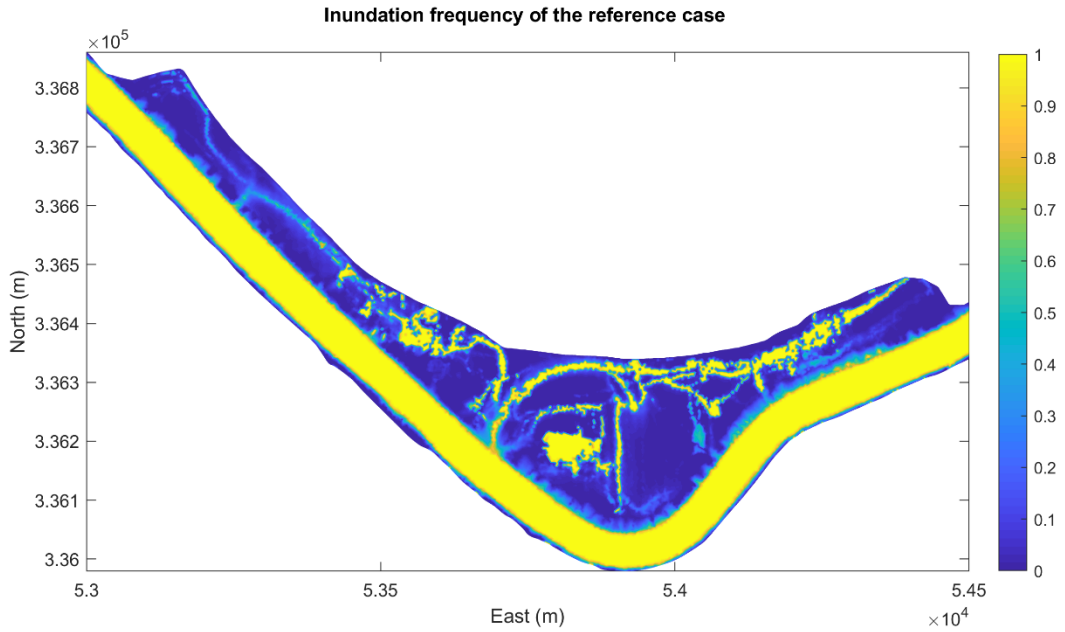

Figure 36 – Inundation frequency of the scenario A

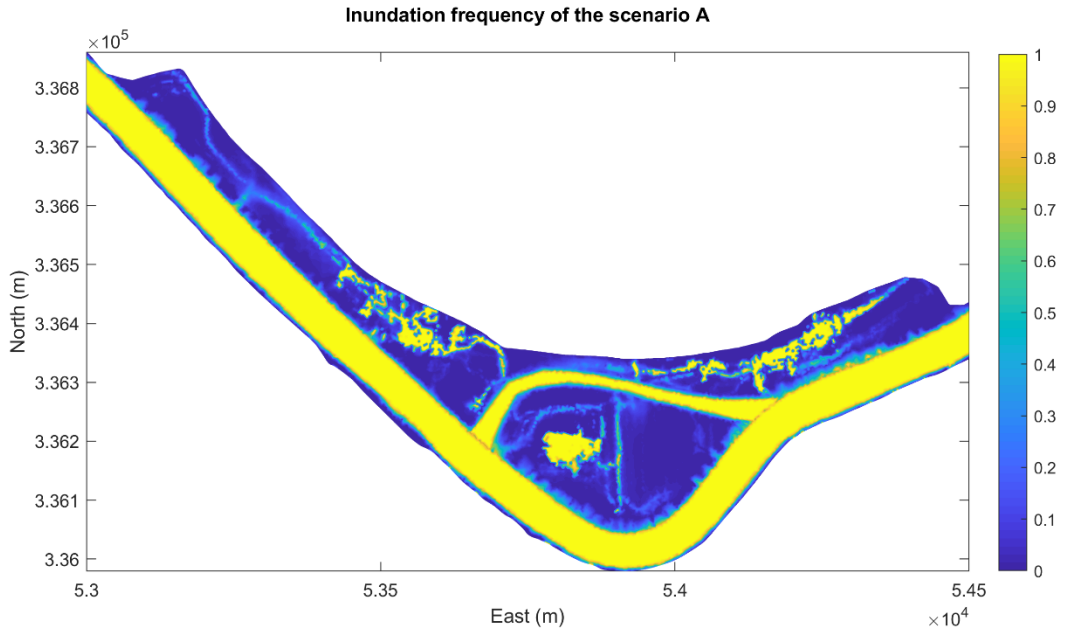

Figure 37 – Inundation frequency of the scenario E1

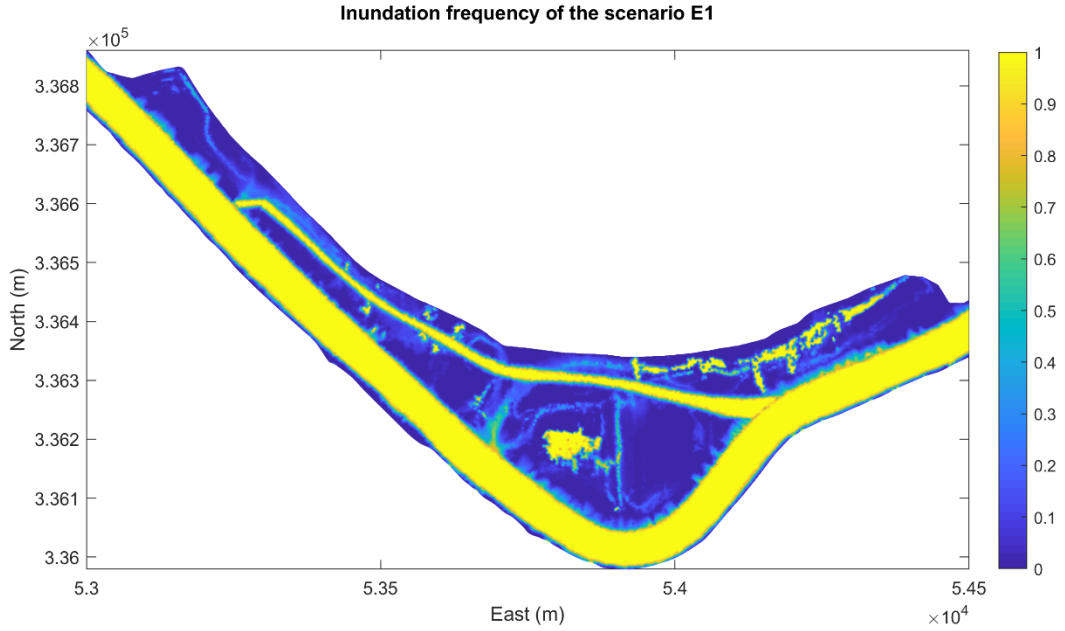

Figure 38 – Inundation frequency of the scenario E2

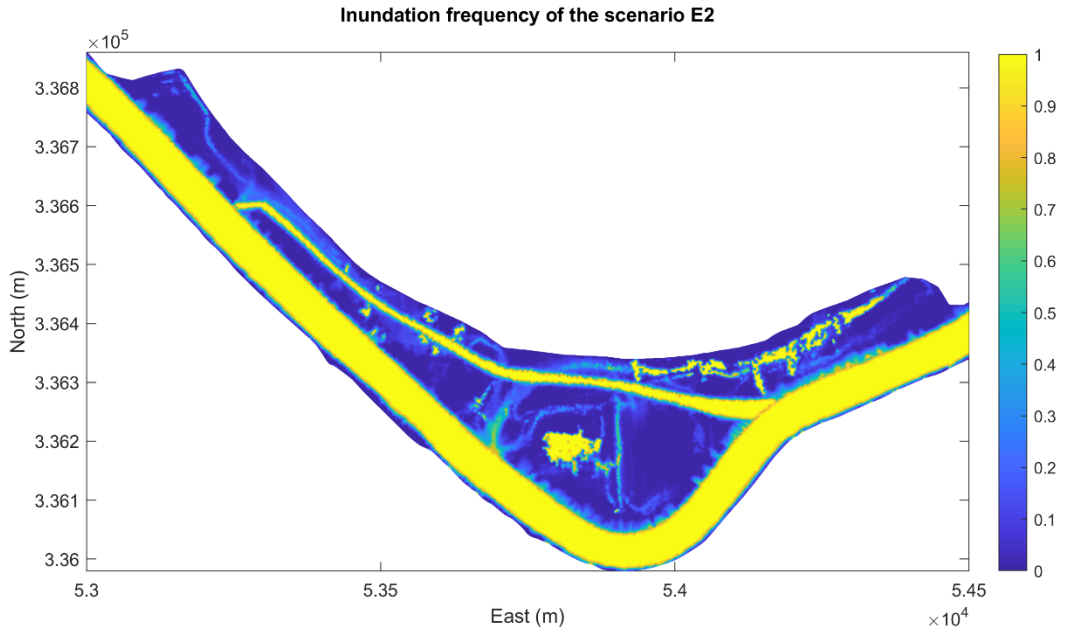

Figure 39 – Inundation frequency of the scenario E3

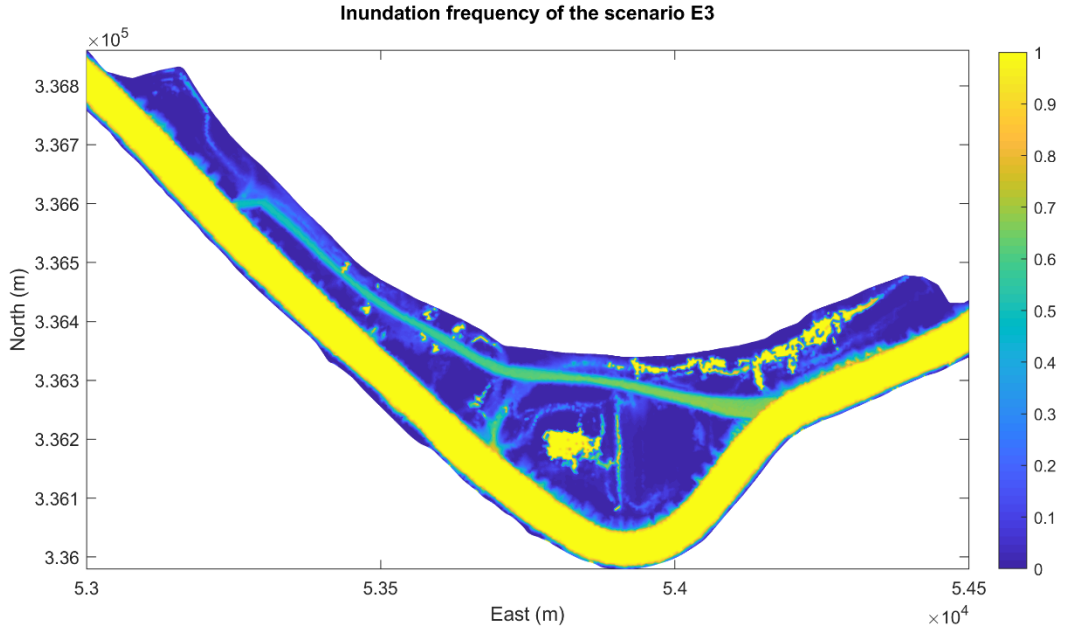

5.3 Tidal amplitude

The average tidal amplitude in the main channel is calculated (Table 4). The amplitude is deduced from the water level differences between high tides and low tides. The location of the transects is indicated in Figure 28.

Table 4 – Comparison of average tidal amplitude at each transect

	Transect 1	Transect 2	Transect 3	Transect 4
Reference	2.802	2.795	2.773	2.762
Scenario A	2.731	2.724	2.700	2.691
Scenario E1	2.705	2.699	2.678	2.667
Scenario E2	2.729	2.722	2.700	2.689
Scenario E3	2.740	2.733	2.710	2.699

Figure 40 – Comparison of average tidal amplitude at each transect for all the scenarios

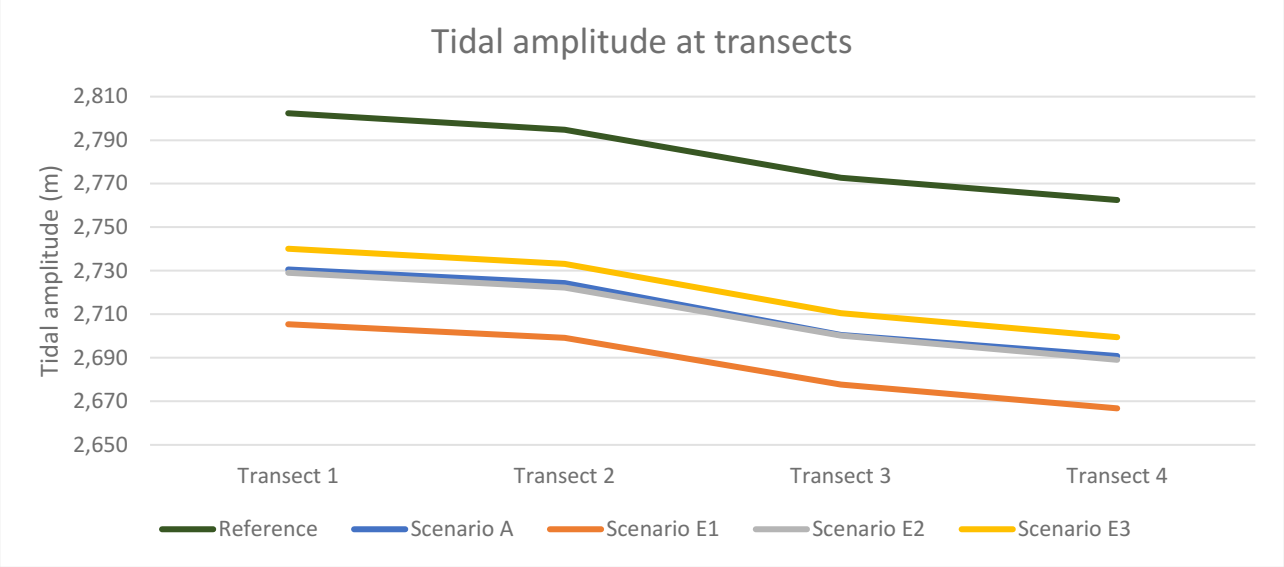

It can be seen in Figure 40 that Scenario E1 gives the lowest amplitude, whereas Scenario E3 gives the highest amplitude. The difference between A and E2 are in small (~2 mm). Based on the current implementation (imposed discharges at both upstream and downstream boundaries), the tidal amplitude is reduced by maximum 10cm in the scenario E1. This is similar as found in the 1D model developed in IMDC.

It is worth pointing out that the magnitude of the reduced tidal amplitude is also dependent on the type of boundary conditions. But the relative differences between the scenarios should be consistent under different set of boundary conditions.

5.4 Flow velocity

The depth-averaged velocity in all the scenarios can be seen in Figure 42 - Figure 45. The velocity field at two moments, one during the flood phase (04/08/2013 04:20:00) and the other one during the ebb phase (04/08/2013 07:20:00), are plotted for showing the different flow patterns in the channels and on the floodplain.

Figure 41 – The flow velocity in the reference case during the flood phase (04/08/2013 04:20:00, upper panel), and during the ebb phase (04/08/2013 07:20:00, lower panel)

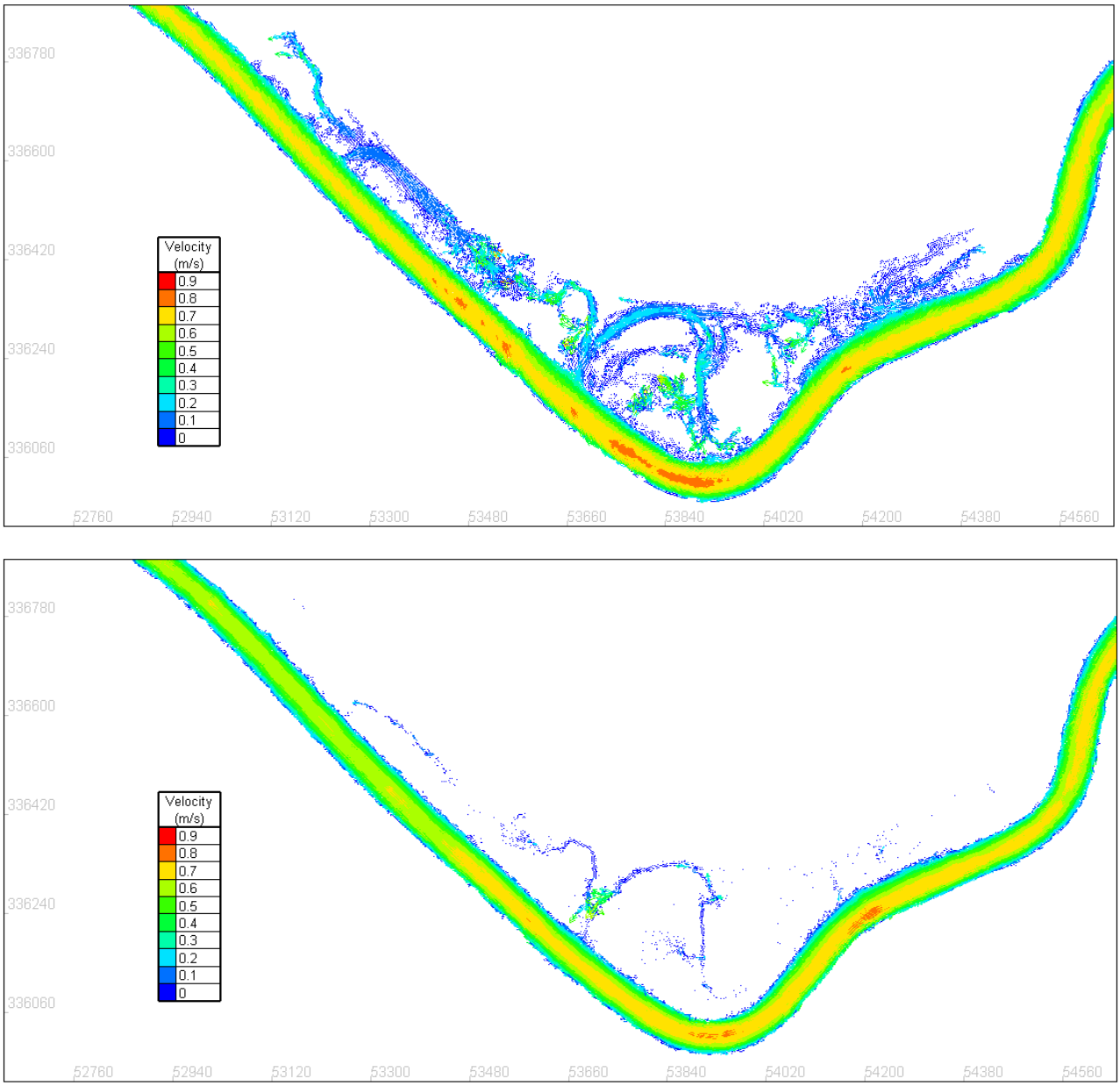

Figure 42 – The flow velocity in Scenario A during the flood phase (04/08/2013 04:20:00, upper panel), and during the ebb phase (04/08/2013 07:20:00, lower panel)

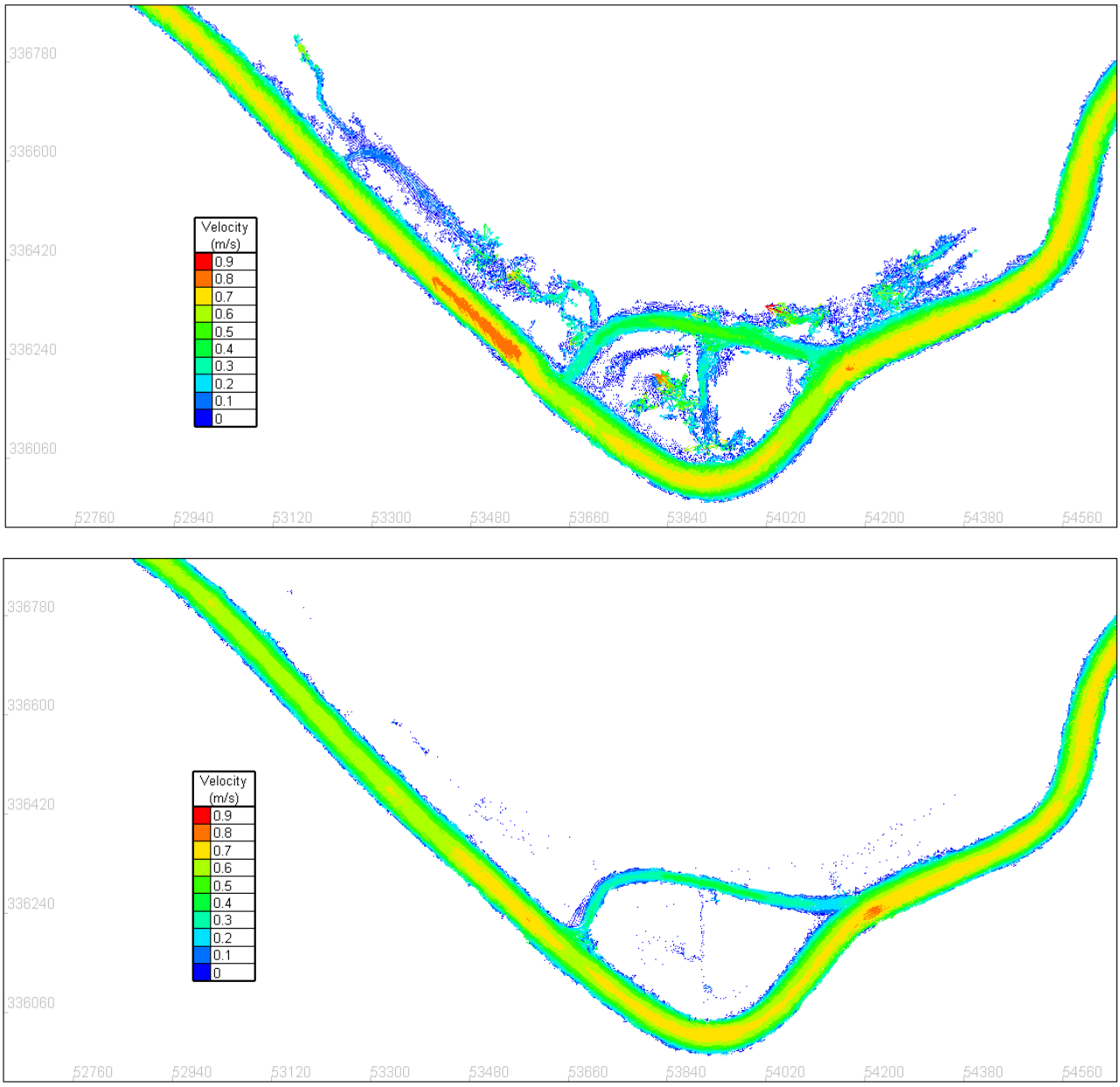

Figure 43 – The flow velocity in Scenario E1 during the flood phase (04/08/2013 04:20:00, upper panel), and during the ebb phase (04/08/2013 07:20:00, lower panel)

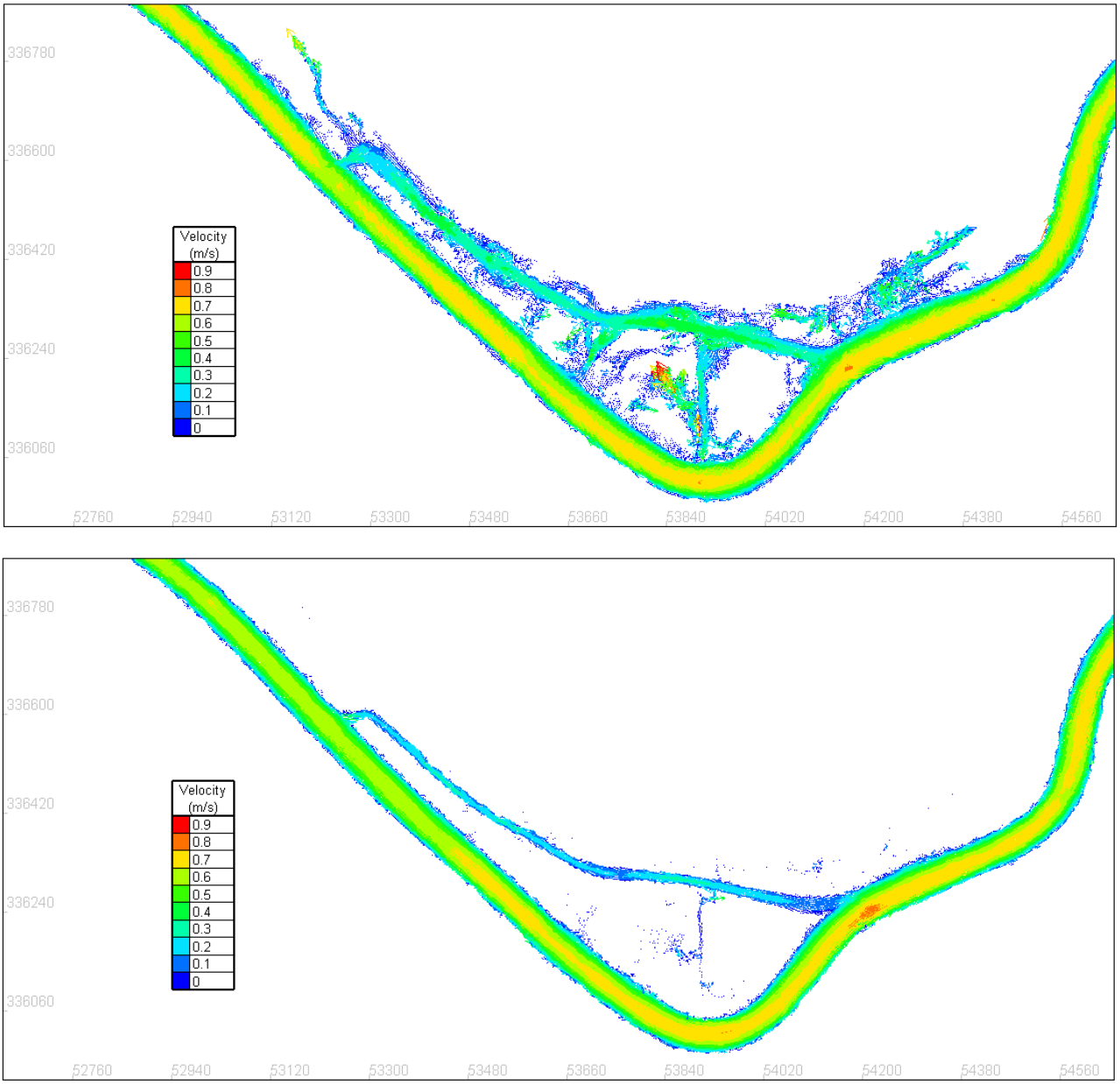

Figure 44 – The flow velocity in Scenario E2 during the flood phase (04/08/2013 04:20:00, upper panel), and during the ebb phase (04/08/2013 07:20:00, lower panel)

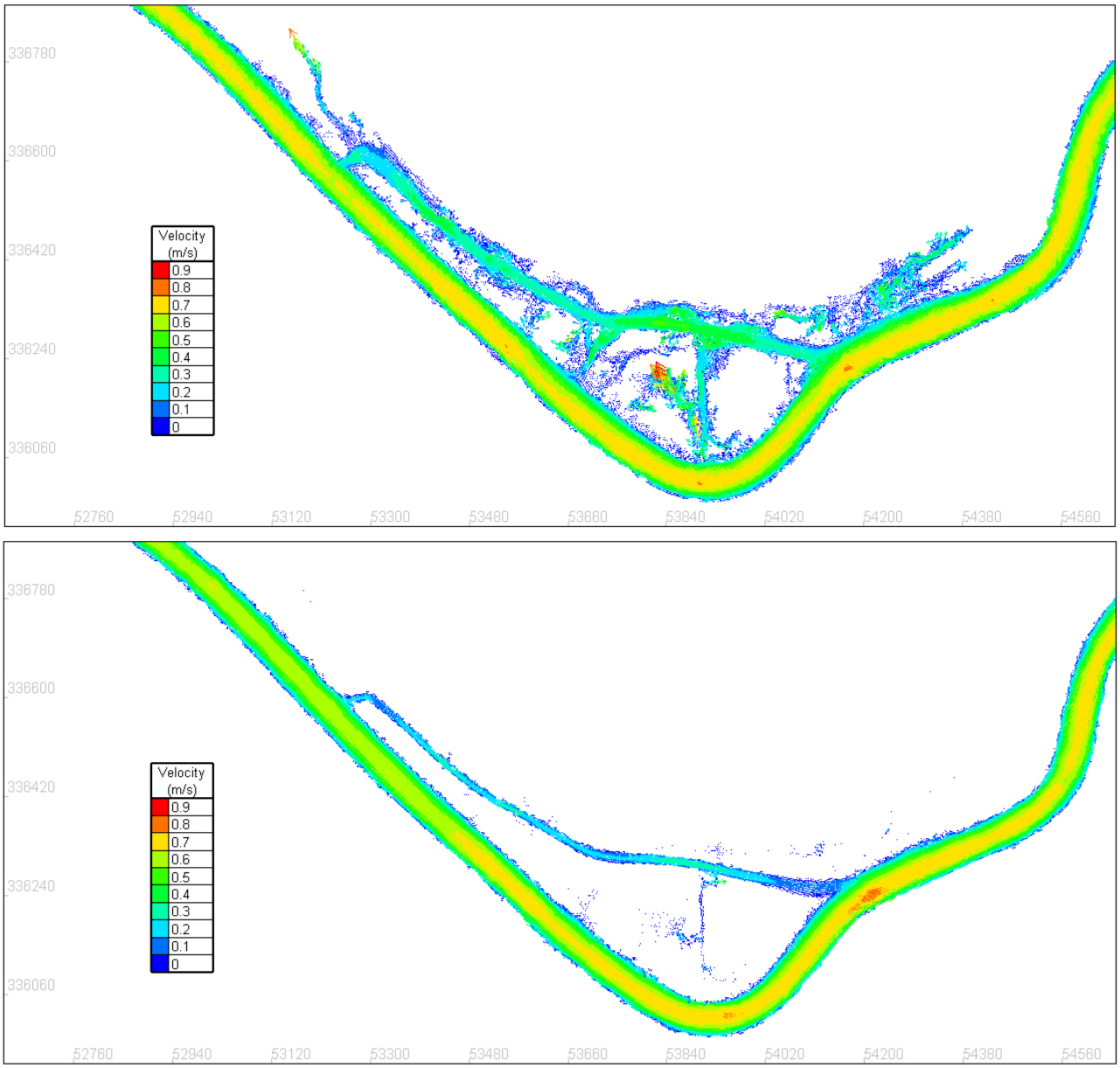

Figure 45 – The flow velocity in Scenario E3 during the flood phase (04/08/2013 04:20:00, upper panel), and during the ebb phase (04/08/2013 07:20:00, lower panel)

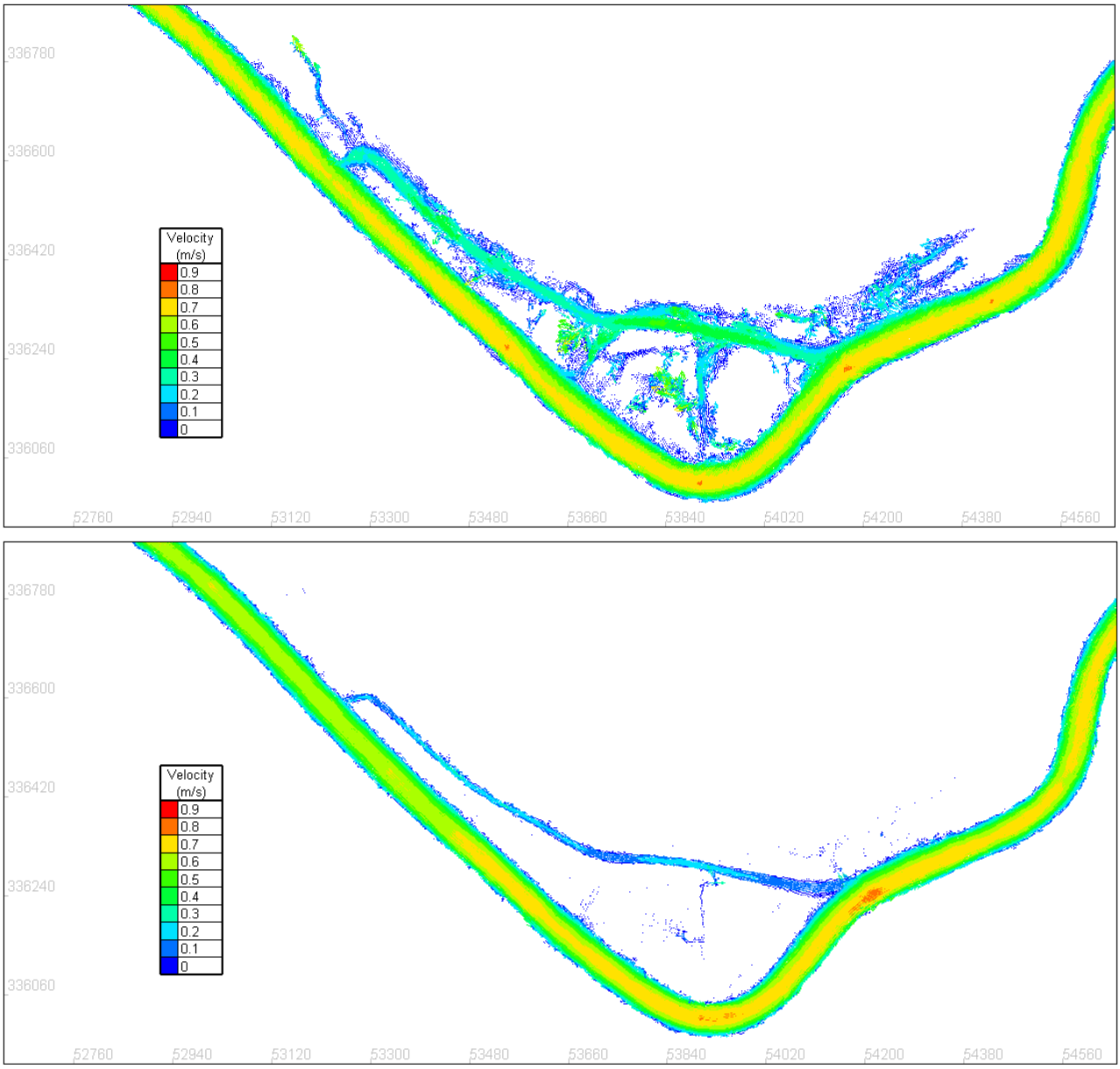

The cross-sectionally averaged velocity is also calculated from the results at each transect. The location of the transects is indicated in Figure 19.

Positive (negative) values mean the velocity is directed downstream (upstream).

Figure 46 – Comparison of cross-sectionally averaged velocity at transects 2.
Positive (negative) values mean the velocity is directed downstream (upstream)

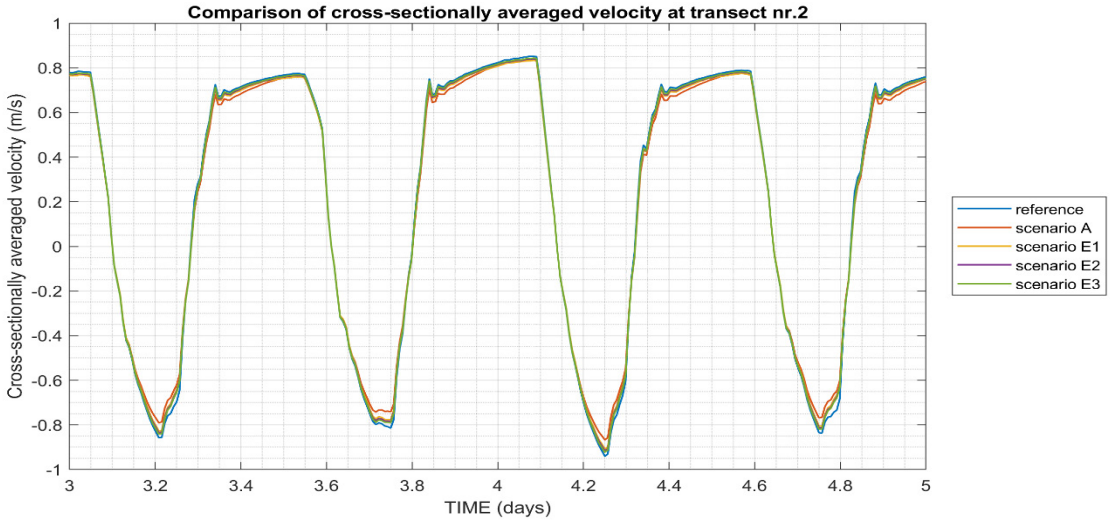

Figure 47 – Comparison of cross-sectionally averaged velocity at transects 5.
Positive (negative) values mean the velocity is directed downstream (upstream)

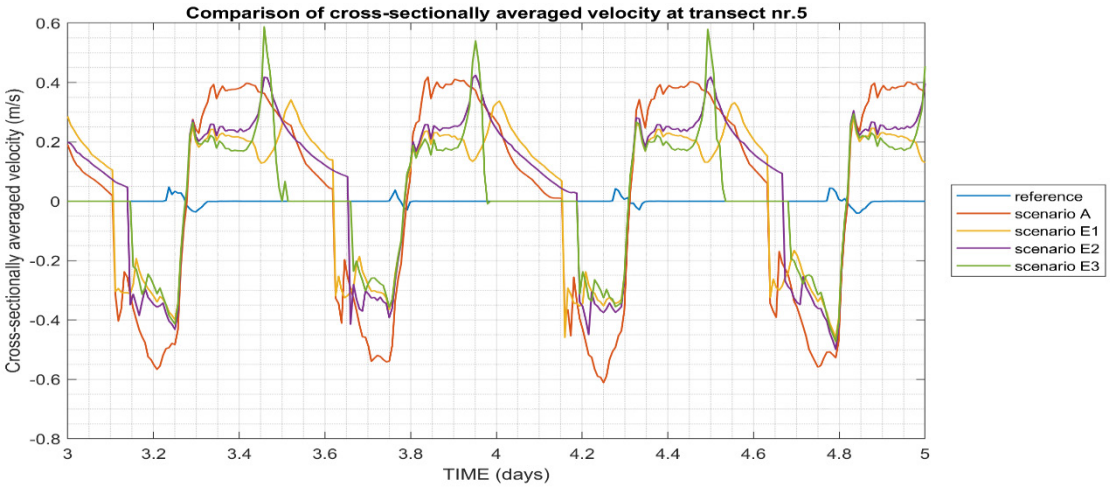

Figure 48 – Comparison of cross-sectionally averaged velocity at transects 6.
Positive (negative) values mean the velocity is directed downstream (upstream)

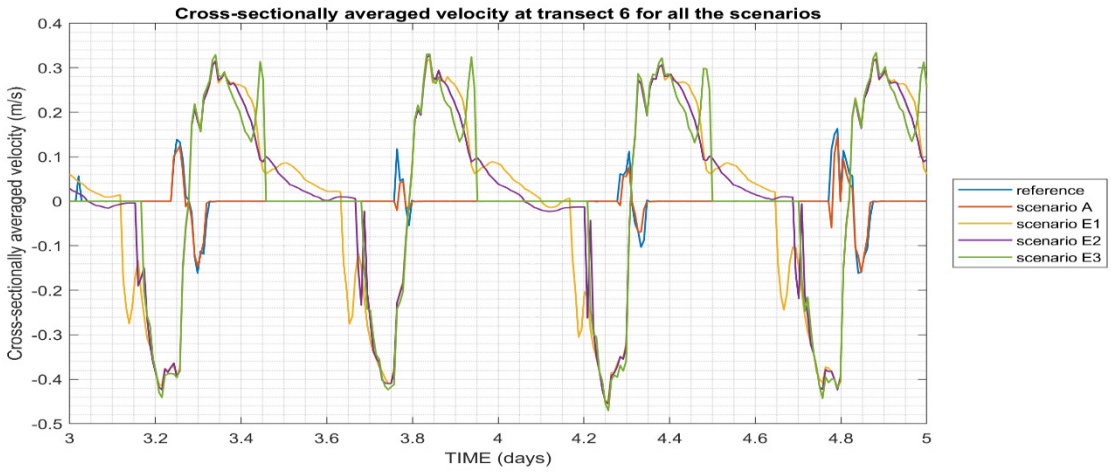

Figure 49 – Comparison of cross-sectionally averaged velocity at transects 7.
Positive (negative) values mean the velocity is directed downstream (upstream)

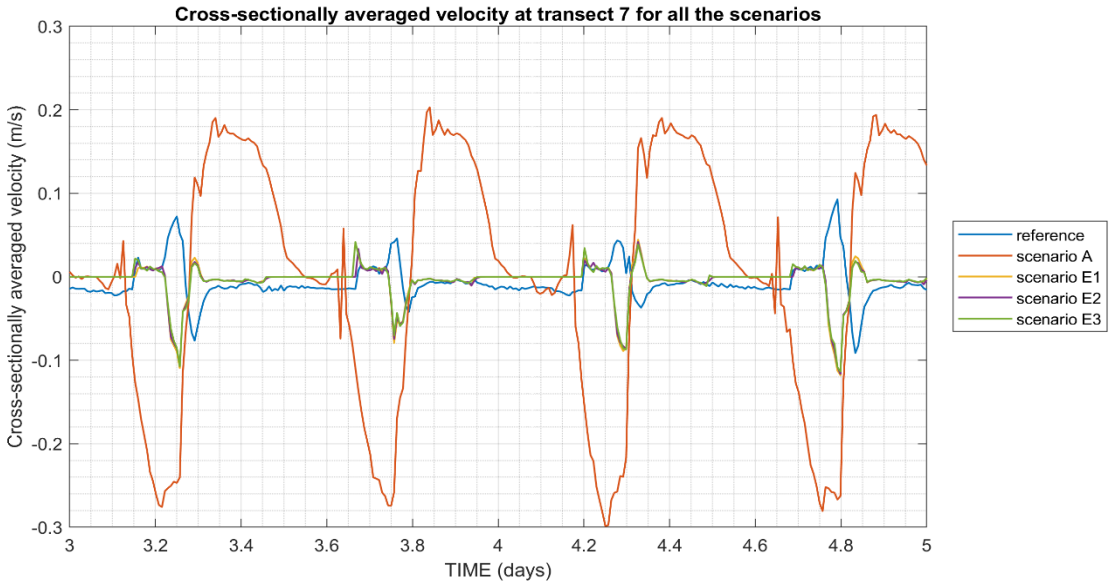

As shown in Table 5, the maximum velocity magnitude in the secondary channel has the largest value at the transect 5. In all the scenarios, A has the largest velocity magnitude, which is 0.611 m/s at transect 5. For the upstream extension of the secondary channel in all the scenarios (transect 6), the largest velocity magnitude is found in the Scenario E3, which is about 0.470 m/s. For the downstream outflow of the secondary channel (transect 7), the maximum velocity magnitude is found in the Scenario A, which is about 0.30 m/s.

Table 5 – The maximum cross-sectionally velocity magnitude (m/s) at each transect for each scenario

	Transect 1	Transect 2	Transect 3	Transect 4	Transect 5	Transect 6	Transect 7
Reference	0.849	0.940	0.788	0.803	0.045	0.164	0.093
Scenarios A	0.856	0.867	0.787	0.804	0.611	0.160	0.299
Scenarios E1	0.859	0.908	0.761	0.803	0.460	0.452	0.118
Scenarios E2	0.858	0.916	0.769	0.803	0.499	0.455	0.116
Scenarios E3	0.859	0.923	0.775	0.803	0.579	0.470	0.114

5.5 Bottom shear stress

The bottom shear stress is computed from the shear velocity given in the results according to the definition

$$\tau_b = \rho u_*^2 \tag{2}$$

where τ_b is the bottom shear stress, ρ is the water density and u_* is the shear velocity.

The calculated bottom shear stress and its spatial-temporal patterns in all the four scenarios are then plotted in Figure 51 to Figure 54, in which two moments, one during the flood phase (04/08/2013 04:20:00) and the other one during the ebb phase (04/08/2013 07:20:00), are shown.

Figure 50 – The bed shear stress in the reference case during the flood phase (04/08/2013 04:20:00, upper panel), and during the ebb phase (04/08/2013 07:20:00, lower panel)

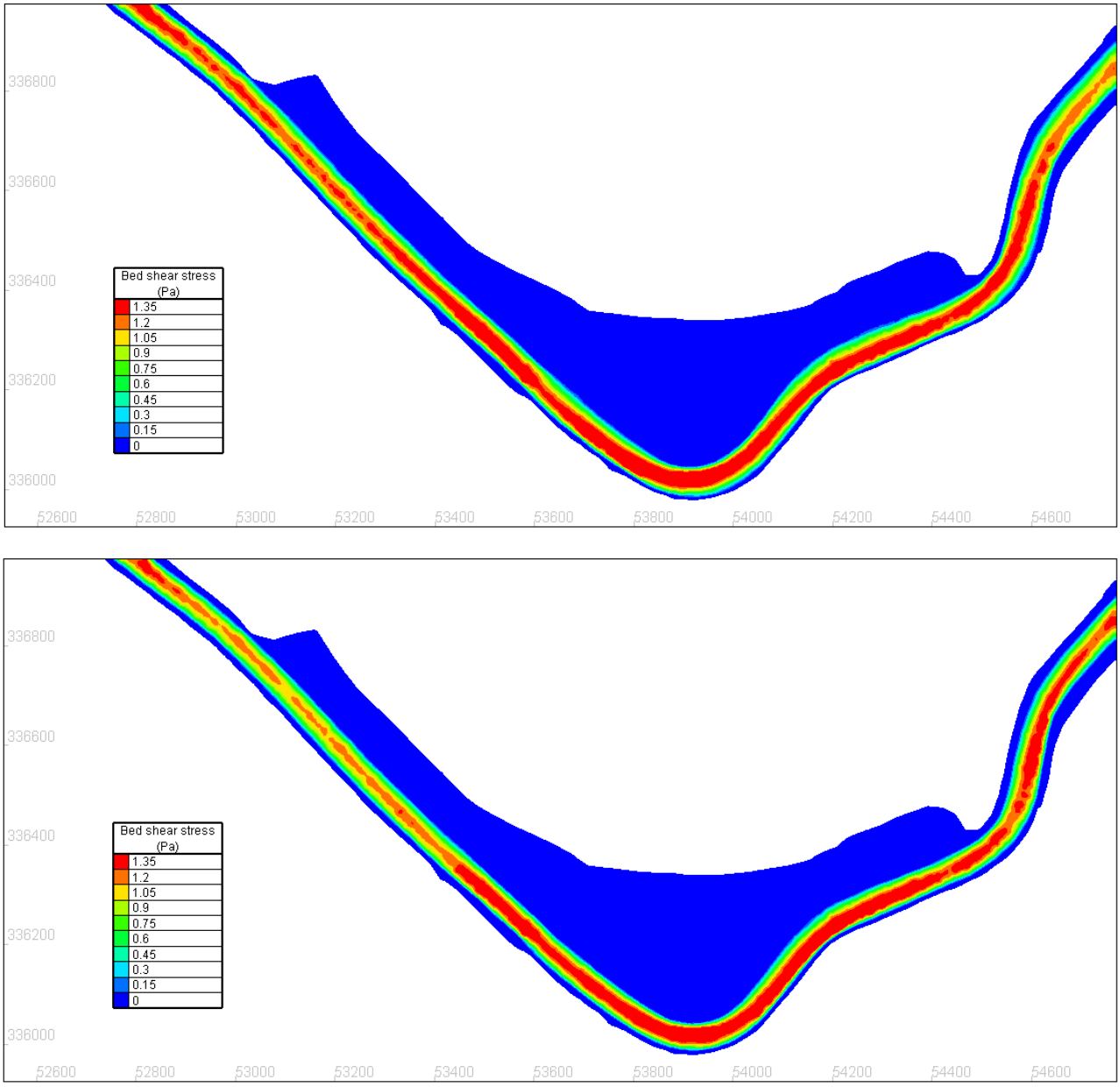

Figure 51 – The bed shear stress in Scenario A during the flood phase (04/08/2013 04:20:00, upper panel), and during the ebb phase (04/08/2013 07:20:00, lower panel)

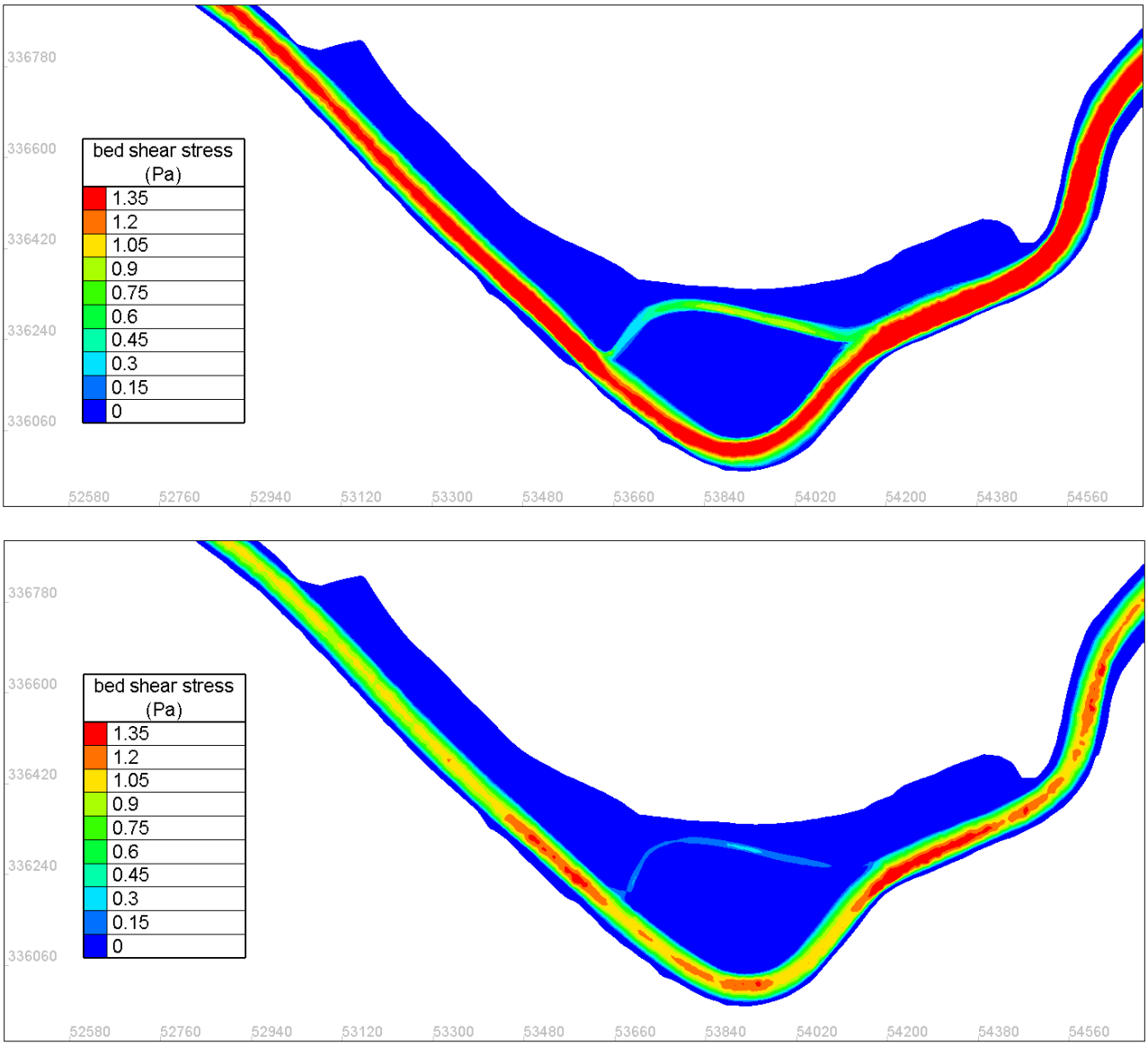

Figure 52 – The bed shear stress in Scenario E1 during the flood phase (04/08/2013 04:20:00, upper panel), and during the ebb phase (04/08/2013 07:20:00, lower panel)

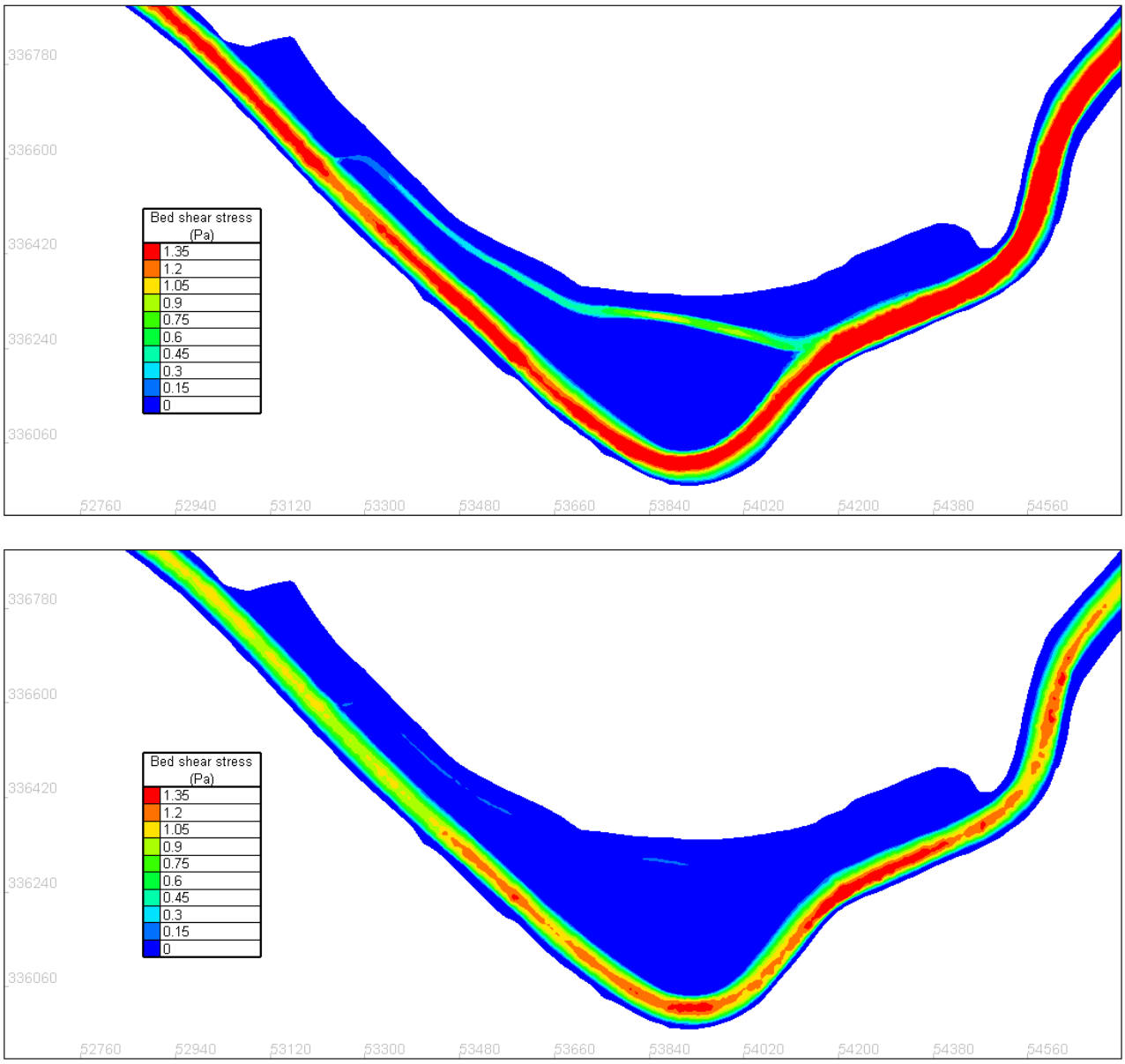

Figure 53 – The bed shear stress in Scenario E2 during the flood phase (04/08/2013 04:20:00, upper panel), and during the ebb phase (04/08/2013 07:20:00, lower panel)

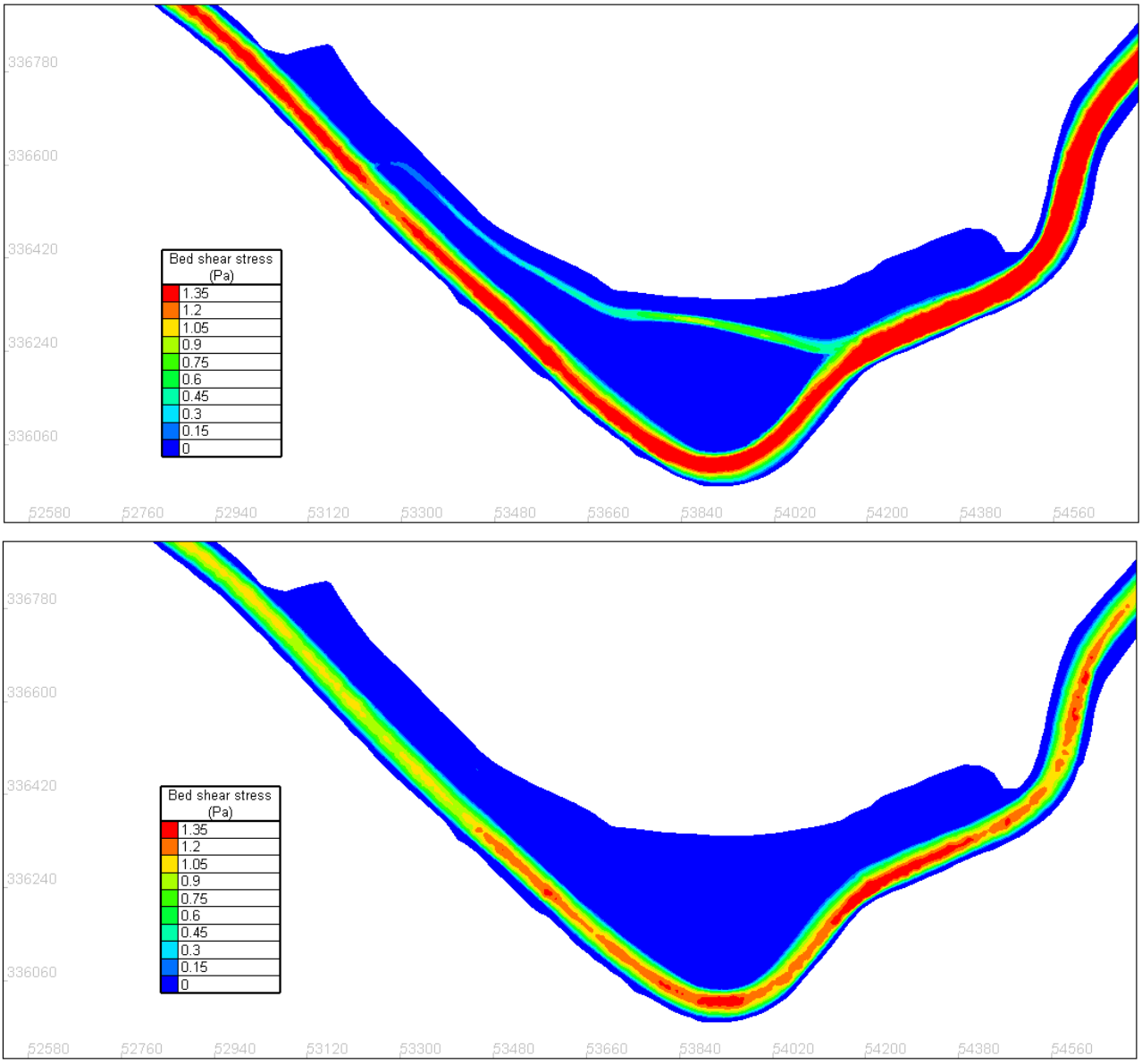

Figure 54 – The bed shear stress in Scenario E3 during the flood phase (04/08/2013 04:20:00, upper panel), and during the ebb phase (04/08/2013 07:20:00, lower panel)

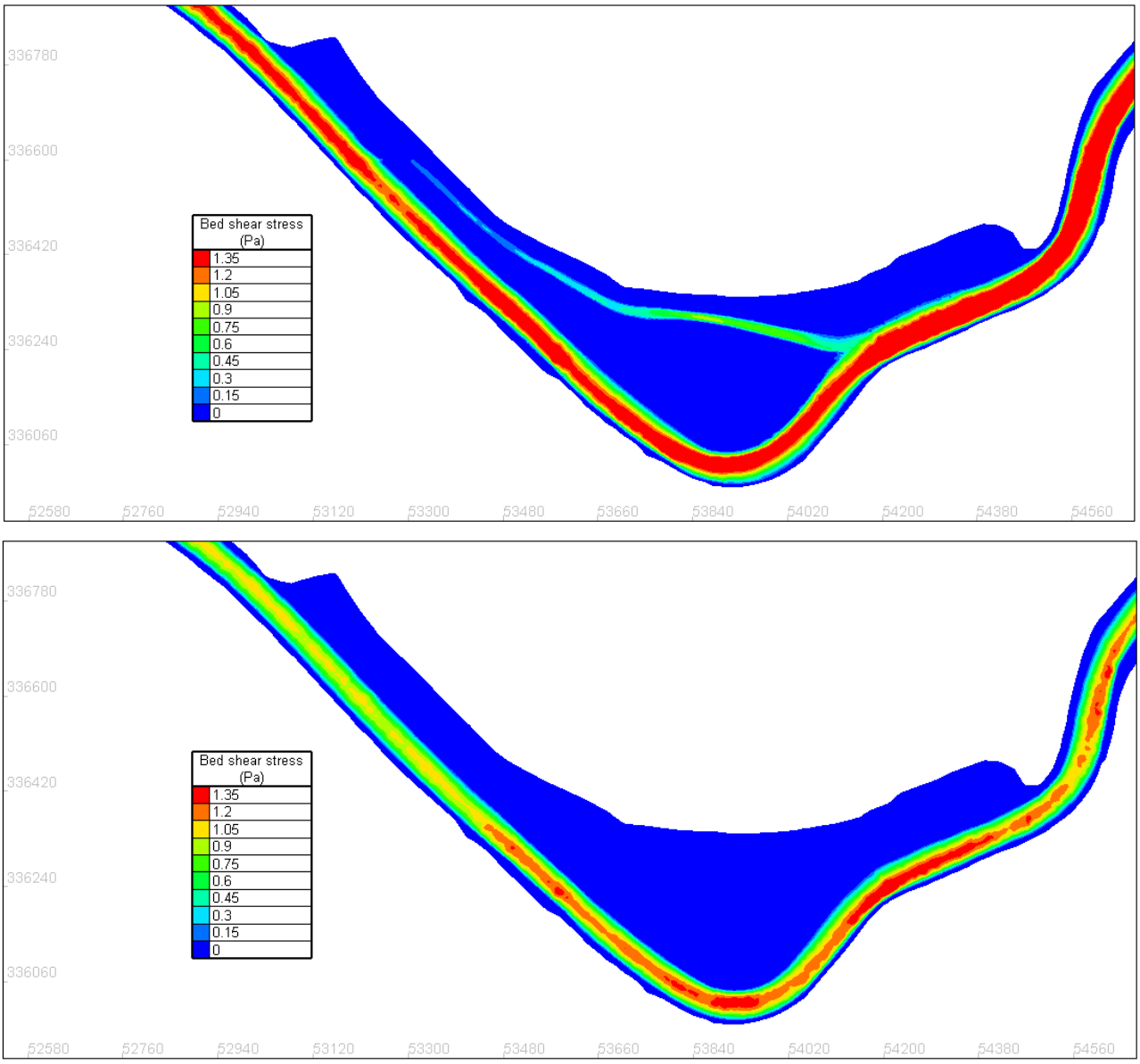

The time series of bottom shear stress at the middle point of each transect is also shown in Figure 55 to Figure 58.

Figure 55 – Comparison of bottom shear stress at the middle point of transect 2

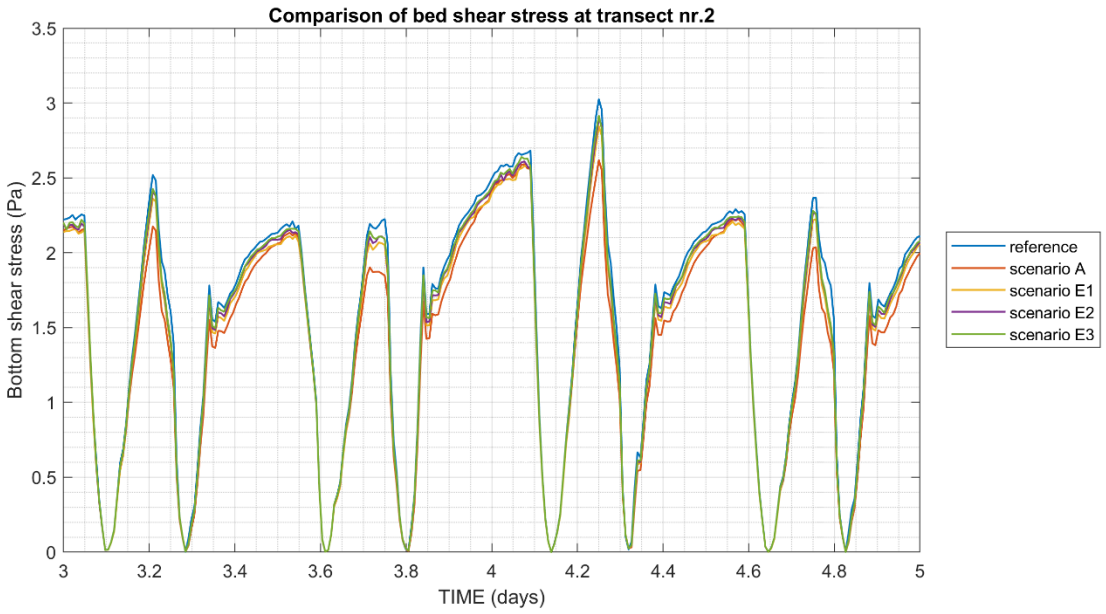

Figure 56 – Comparison of bottom shear stress at the middle point of transect 5

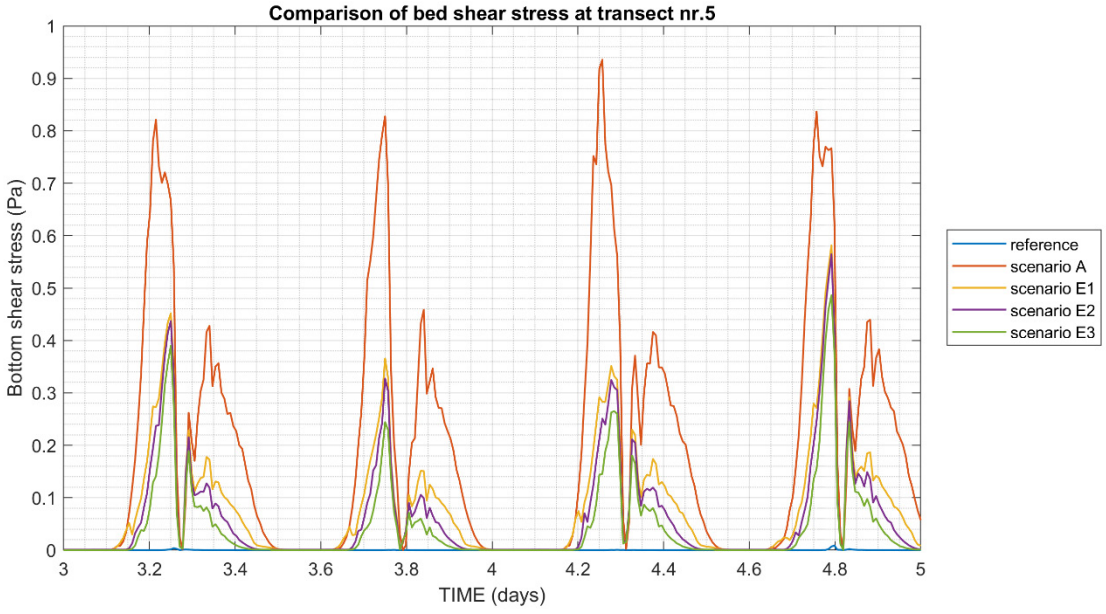

Figure 57 – Comparison of bottom shear stress at the middle point of transect 6

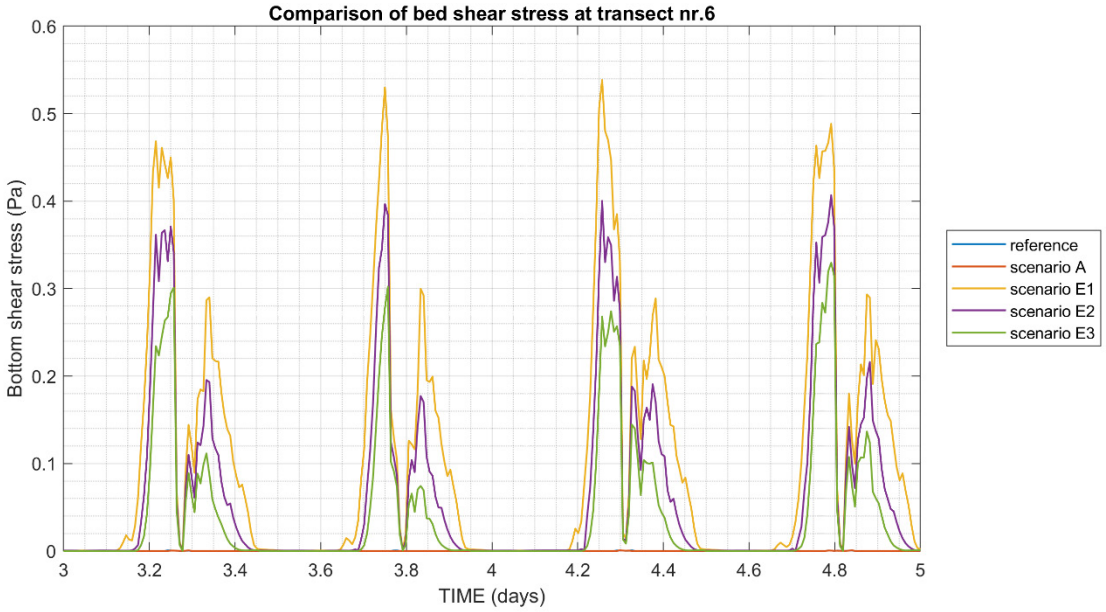

Figure 58 – Comparison of bottom shear stress at the middle point of transect 7

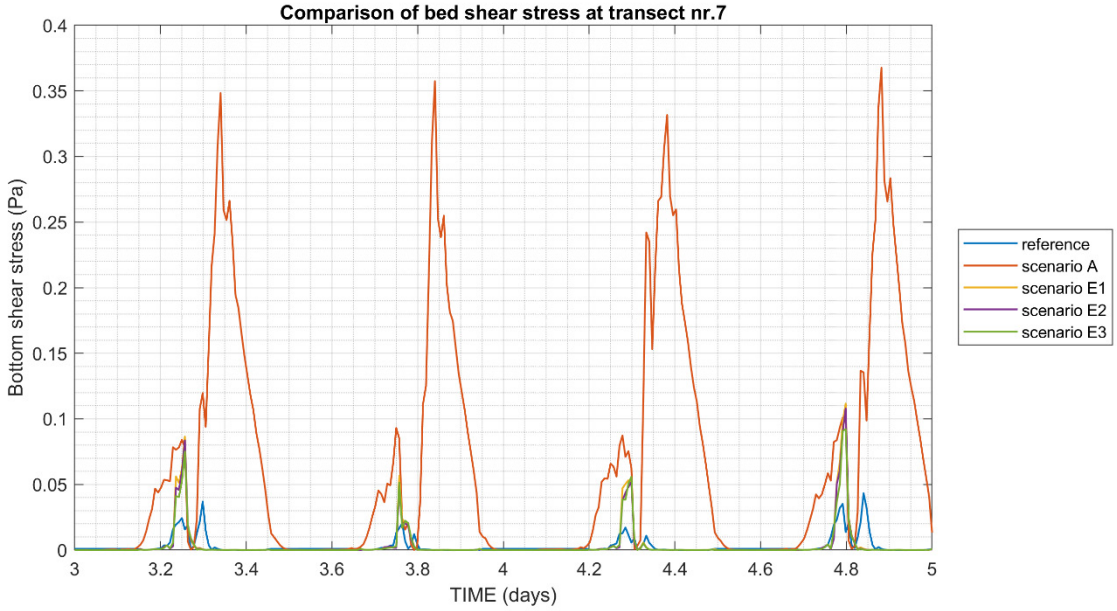

The maximum bottom shear stress at each transect for each scenario is shown in Table 6.

In the secondary channel, the transect 5 (downstream inlet) has the largest bottom shear stress, which ranges from about 0.49 Pa (scenario E3) to 0.94 Pa (scenario A). The extension of the secondary channel in the E-variants has the bottom shear stress ranging from 0.33 Pa (scenario E3) to 0.54 Pa (scenario E1). The downstream outflow of the secondary channel (transect 7) has the largest value in scenario A, which is about 0.37 Pa. It decreases to the range 0.09 to 0.11 Pa in all the E-variants.

Table 6 – The maximum bottom shear stress (Pa) at each transect for each scenario

	Transect 1	Transect 2	Transect 3	Transect 4	Transect 5	Transect 6	Transect 7
Reference	2.554	3.025	2.565	2.339	0.009	0.001	0.043
Scenarios A	2.604	2.618	2.614	2.345	0.935	0.001	0.368
Scenarios E1	2.615	2.844	2.374	2.361	0.581	0.539	0.112
Scenarios E2	2.620	2.895	2.436	2.366	0.565	0.407	0.108
Scenarios E3	2.622	2.914	2.471	2.360	0.486	0.330	0.092

5.6 Suspension capacity

The suspension capacity indicates the amount of sediment that can be kept in suspension due to the combination effects of turbulence kinetic energy and gravitational settling.

Based on the study of Toorman (2000) and Bi & Toorman (2015), the suspension capacity can be computed from the following equation:

$$C_{sc} = \frac{R_f}{(1-\rho/\rho_s)gH}\frac{U}{w_s}\tau_b \tag{3}$$

where C_{sc} is the suspension capacity [g/L], R_f is the flux Richardson number for sediment at suspension capacity, which expresses the ratio of suspension potential to turbulent kinetic energy, ρ is the water density [kg/m^3], ρ_s is the sediment density [kg/m^3], which is 1800 kg/m^3 as the representative density of mud found in the Scheldt estuary (Winterwerp, 2004), g is the gravity acceleration [m/s^2], H is the water depth [m], U is the depth-averaged velocity magnitude [m/s], w_s is the settling velocity of sediment particle [m/s], which is assumed to be 2 mm/s in this study, τ_b is the bed shear stress [Pa].

The flux Richardson number can be estimated from the following equation:

$$R_f = 0.25\left(\frac{u_*}{w_s}\right)^2 \cdot \frac{0.01}{1+0.01\left(\frac{u_*}{w_s}\right)^2} \tag{4}$$

where u_* is the shear velocity, w_s is the settling velocity of sediment particle.

Note that the C_{sc} is a function of shear velocity, depth-averaged velocity magnitude and water depth, and it also varies in both time and space. This spatial and temporal variation could give indications about the potential sedimentation in the channels.

However, this suspension capacity represents the maximum depth-averaged concentration, including the high concentration layer near bottom, and it does not obey the mass conservation in the domain, so it is not suitable for estimating the sediment flux or sediment balance in the system.

The suspension capacity is calculated along the secondary channel, in order to evaluate the impact of the scenarios to the morphodynamics – if the secondary channel will stay open or not, and which scenario requires least maintenance. Two kinds of results are given in the sections below for each scenario, the average suspension capacity over ebb period and over flood period, and the snapshots of its spatial patterns at two representative moments - 04/08/2013 04:20:00 (maximum flood discharge in the secondary channel), and 04/08/2013 07:20:00 (maximum ebb discharge in the secondary channel). These will give an overall indication about how the secondary channel will react to the sediment flux in difference scenarios.

5.6.1 Scenario A

The suspension capacity is calculated based on the hydrodynamic results of the scenario A. The suspension capacity is then extracted along the thalweg of the secondary channel as shown in Figure 17. The first point at the inlet is considered as the start point.

The suspension capacity is averaged over ebb and over flood (Figure 59). As seen in the figure, the suspension capacity in the reference is negligible comparing to the scenario A, in which the suspension capacity is higher during flood than during ebb, suggesting that more sediment could be transported during flood.

Figure 59 – Average suspension capacity over ebb and over flood (Scenario A)

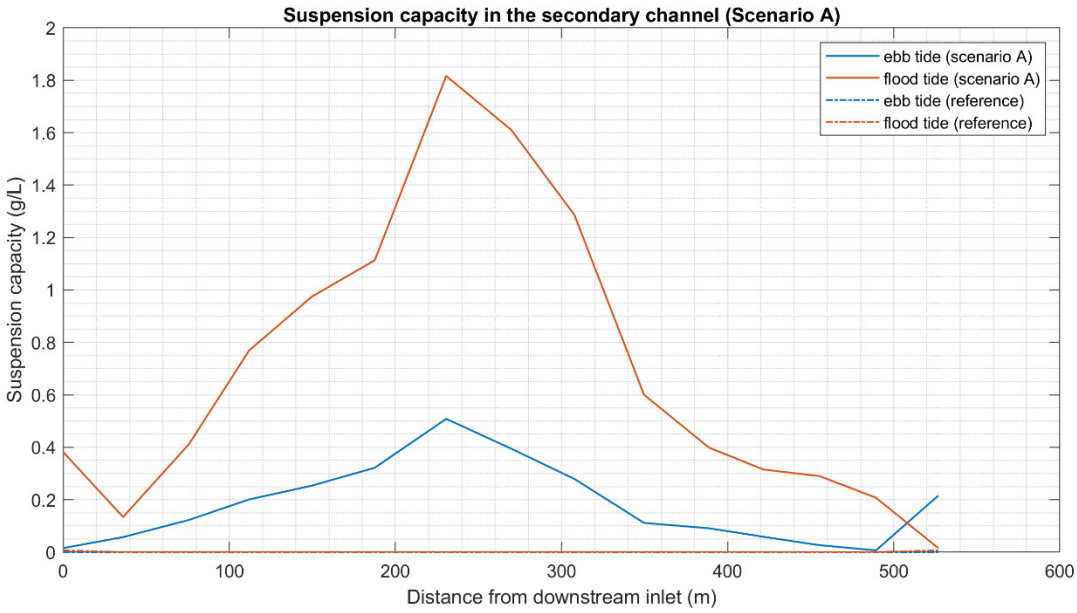

During flood tide, the suspension capacity is higher in the middle of the secondary channel, but lower at inlet and the outflow, implying that if there is enough sediment carried in the main channel, it is possible to have deposition near the inlet, erosion or less deposition in the middle section, and more deposition near the outflow.

The similar trend is also found during the ebb tide. But the difference is that the bed shear stress is much smaller during ebb, meaning that if there is sediment from the main channel, it is most likely to deposit along the secondary channel. These trend can also be confirmed in Figure 60.

Figure 60 – The suspension capacity in Scenario A during the flood phase (04/08/2013 04:20:00, upper panel), and during the ebb phase (04/08/2013 07:20:00, lower panel)

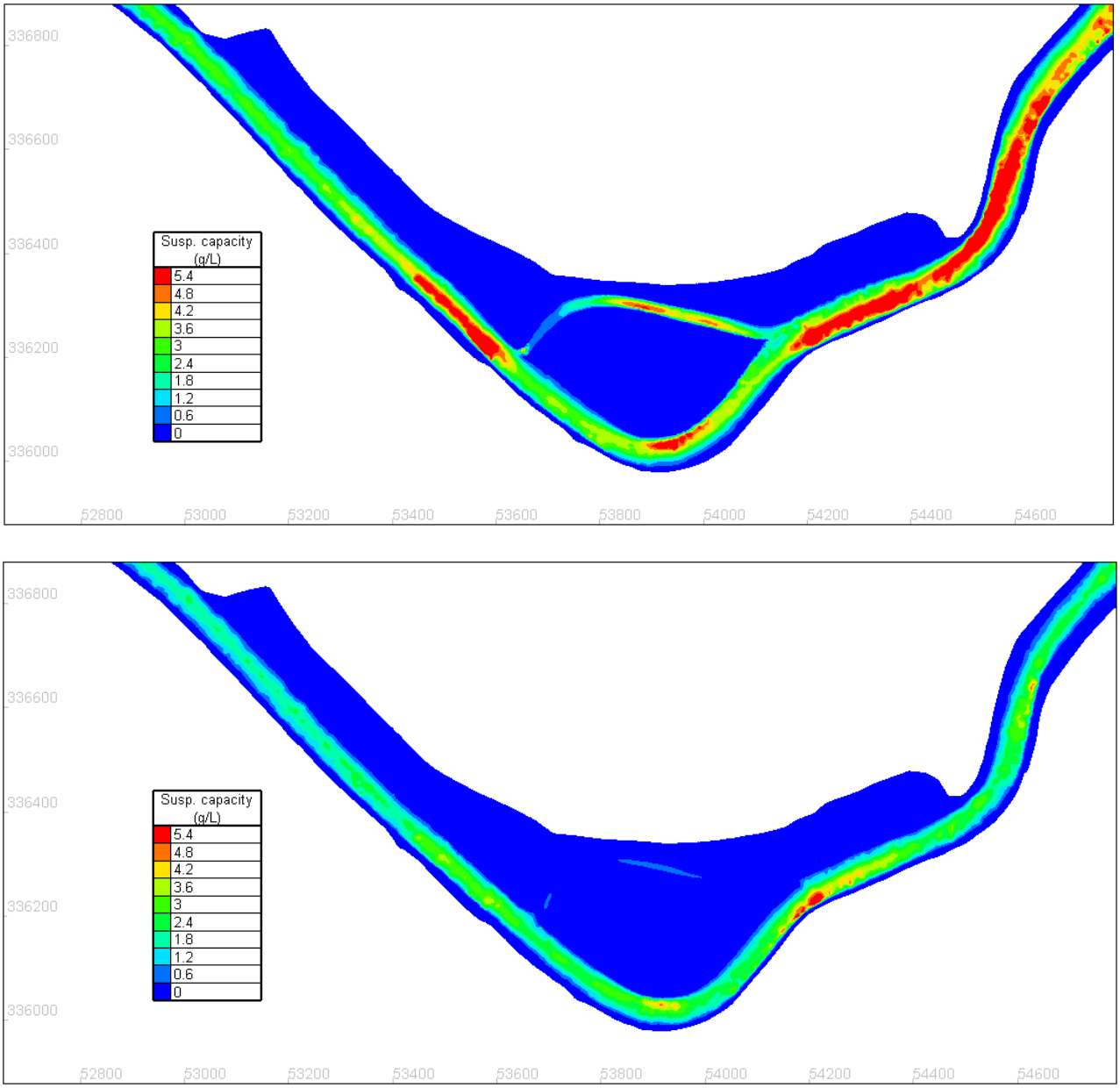

5.6.2 Scenario E

The suspension capacity is calculated based on the hydrodynamic results of all the scenario E-variants. The suspension capacity is then extracted along the thalweg of the secondary channel as shown in Figure 19. The first point at the downstream inlet is considered as the start point.

Here shows the suspension capacity averaged over ebb and over flood. As seen in Figure 61, the suspension capacity in the reference case is negligible, whereas it is much larger in the E scenarios. In the E scenarios, the suspension capacity is higher during flood than during ebb, which again implies that more sediment could be transported during flood.

Figure 61 – Average suspension capacity over ebb and over flood along the secondary channel from the downstream inlet to the upstream outflow (Scenario E-variants)

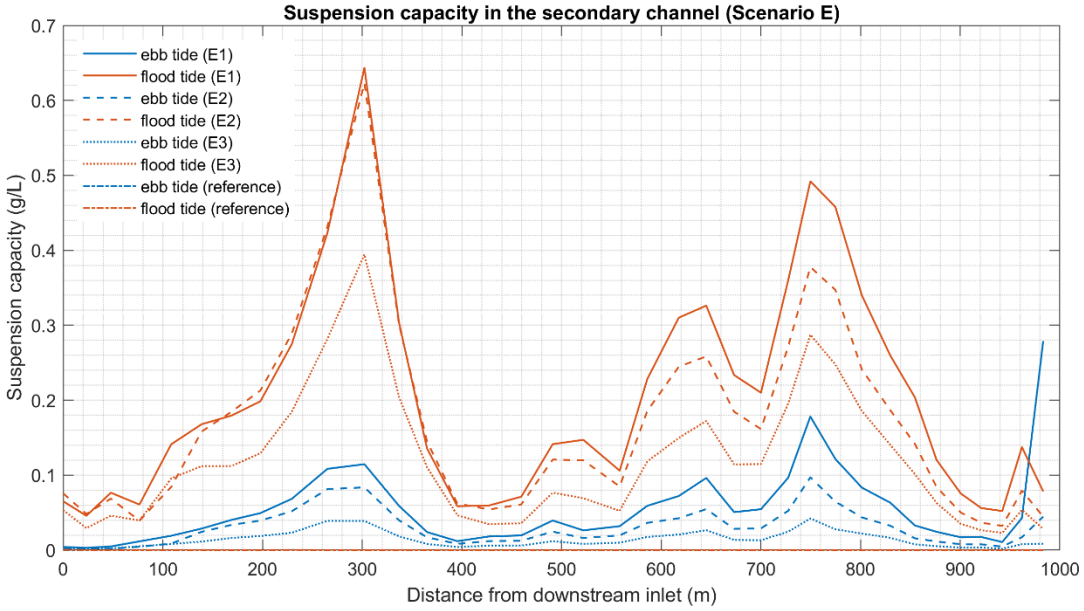

Figure 62 – Average suspension capacity over ebb and over flood along the secondary channel near the downstream outflow (Scenario E-variants)

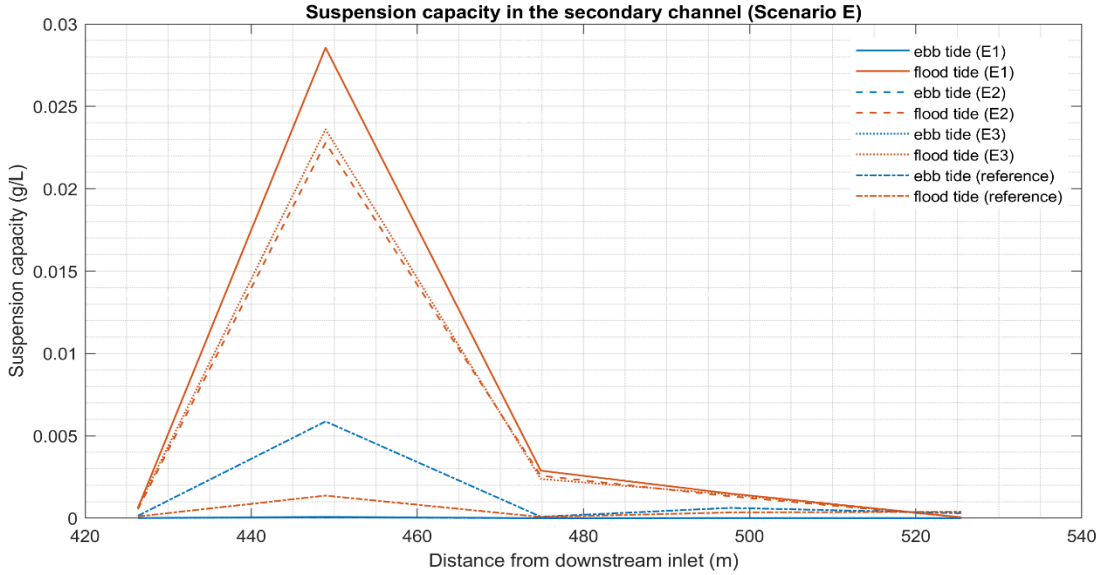

More specifically, during the flood tide, the suspension capacity only shows small differences at the downstream inlet between the scenarios E1 and E2, whereas E3 has lower suspension capacity compared to the other two. But for the extension of the secondary channel towards upstream (400 m – about 1000 m), the differences are obvious. Due to the most elevated bottom at the upstream outflow in the scenario E3 (3 m), the suspension capacity decreases as well, being the least among the three E-variants. For the downstream outflow (about 500 m - 520 m in Figure 62), all the E-variants give the much smaller suspension capacity compared to that in the main channel. This could mean the natural situation in this part of the channel is likely to be kept.

During the ebb tide at the upstream outflow, the highest suspension capacity is found in the scenario E1, due to its lowest bottom elevation among the E-variants. But it decreases also the most significantly in E1 towards the downstream inlet. Hence, the upstream outflow is more likely to be closed in E1 comparing to E2 and E3. On the other hand, the downstream outflow is likely to be well kept since the suspension capacity is low and it will be deposited before reaching to this outflow.

The snapshots of the suspension capacity, bed shear stress and velocity for each E-variant are shown below.

Figure 63 – The suspension capacity in Scenario E1 during the flood phase (04/08/2013 04:20:00, upper panel), and during the ebb phase (04/08/2013 07:20:00, lower panel)

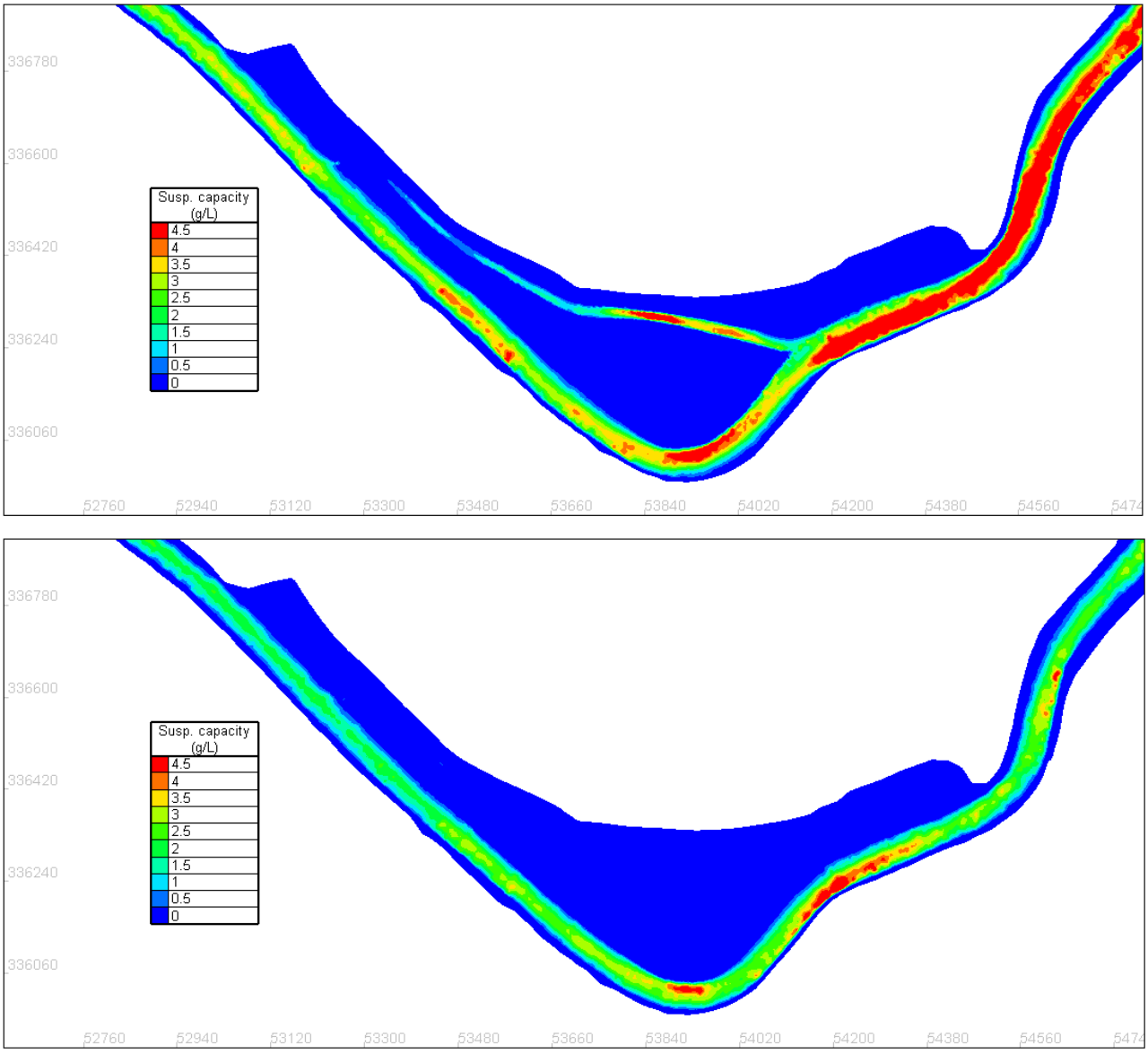

Figure 64 – The suspension capacity in Scenario E2 during the flood phase (04/08/2013 04:20:00, upper panel), and during the ebb phase (04/08/2013 07:20:00, lower panel)

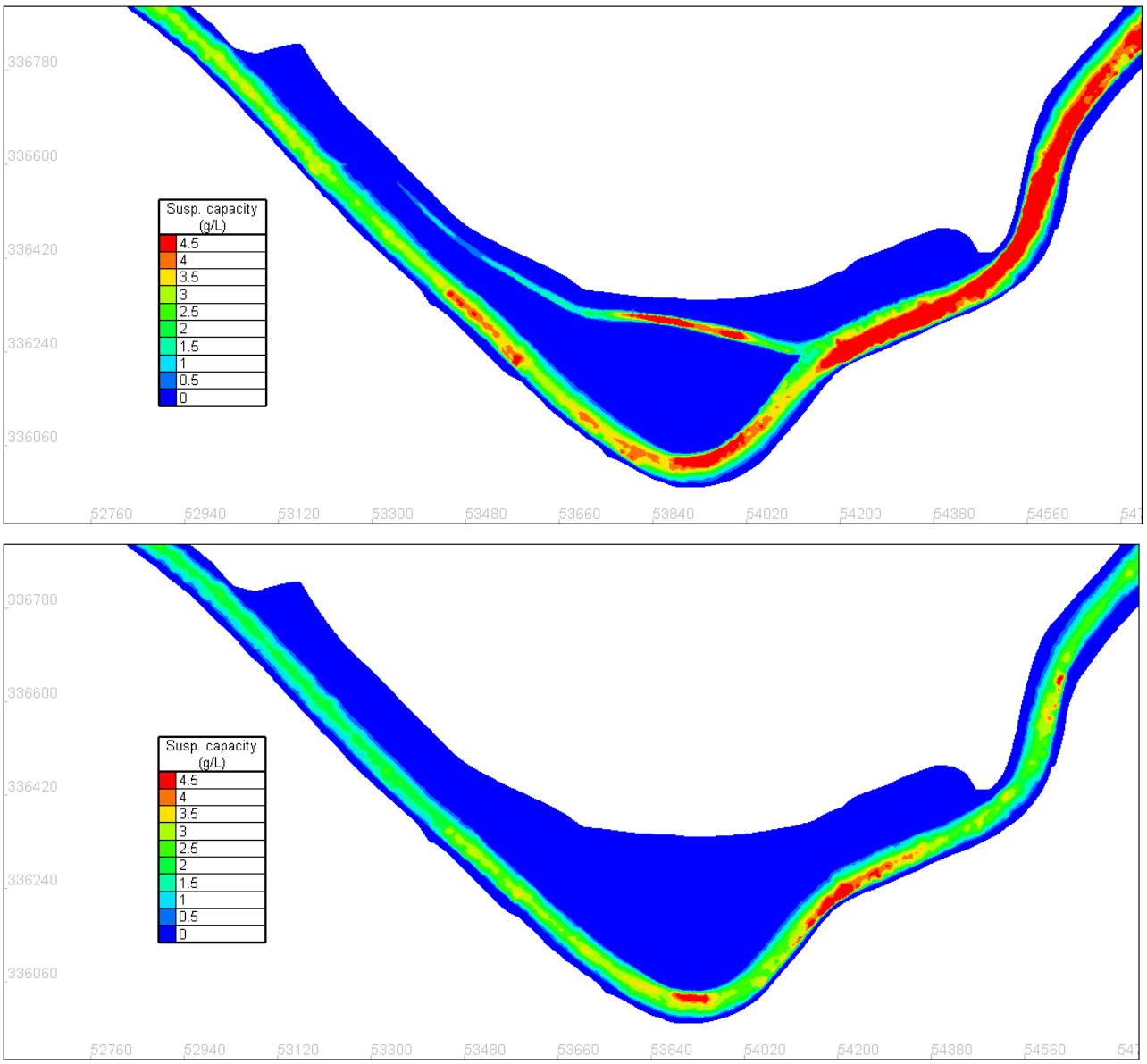

Figure 65 – The suspension capacity in Scenario E3 during the flood phase (04/08/2013 04:20:00, upper panel), and during the ebb phase (04/08/2013 07:20:00, lower panel)

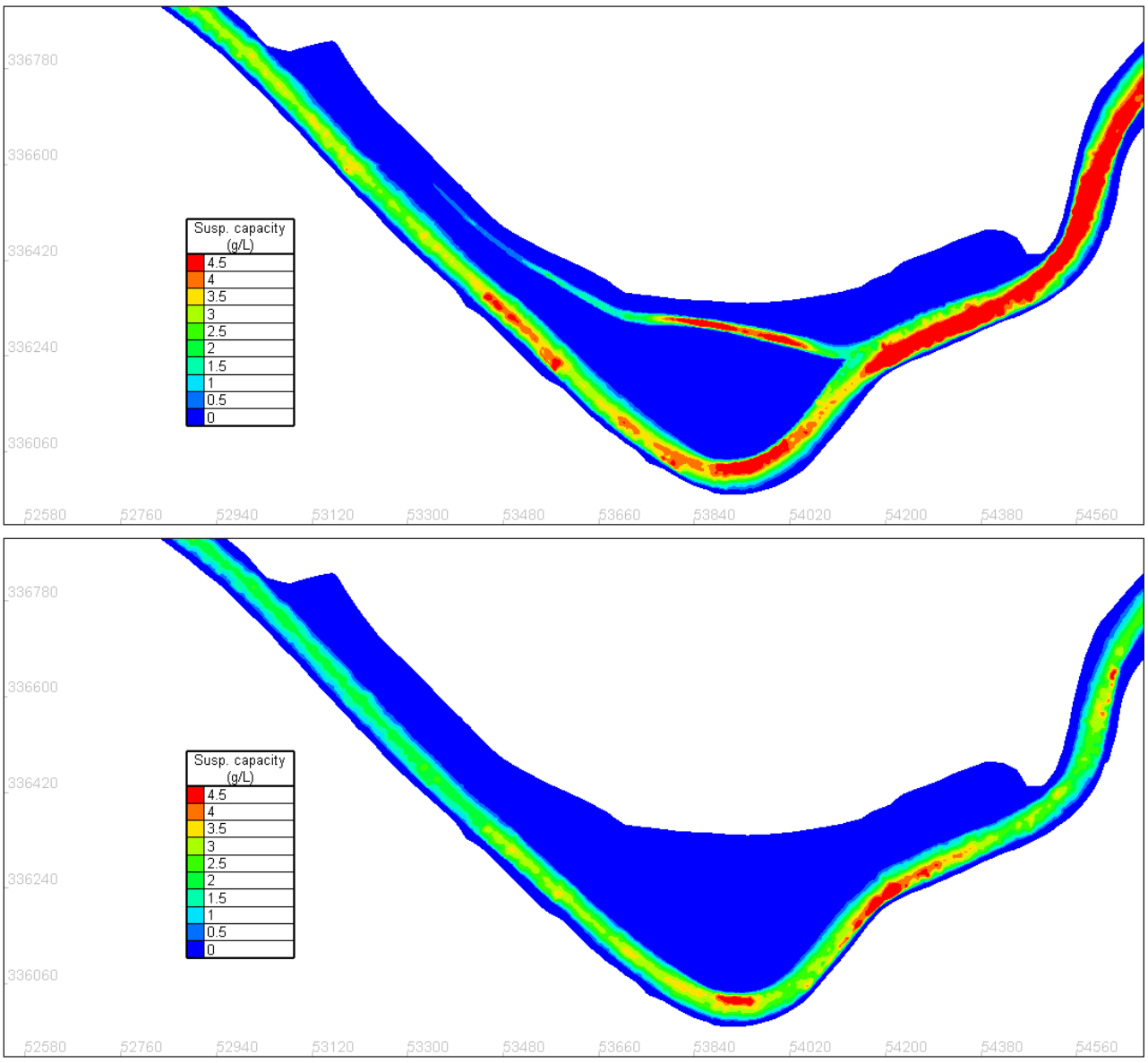

6 Conclusions

For the discharge, it is suggested that the discharge in the secondary channel is about 5% – 10 % of the total discharge. According to the simulation results, the discharge in the secondary channel in all the scenarios are within 10% of the total discharge. More specifically, scenario A has the highest ratio of about 7% during ebb and 10% during flood, while scenario E3 has the lowest ration about 5% during ebb and 6% during flood. It is worth mentioning that the largest differences among the E scenarios are between E1 and E3, which is about 2% in average.

One of the function of the secondary channel is to providing protection against flood by reducing the tidal amplitude. This aspect is also assessed in the model. The results show that scenario E1 has the lowest tidal amplitude in the main channel, which is about 3.5cm lower than the highest scenario E3. Scenario A and E2 have similar tidal amplitude, which is about 1.0cm lower than the scenario E3.

The design criterial also requires the flow velocity to cover the entire range of 0.10-0.80 m/s in order to be low enough to prevent erosion of the bed and bank erosion, but still high enough to satisfy the ecological targets. In the model results, scenario A covers the widest velocity range (about 0.0 – 0.61m/s), whereas E1 has the narrowest velocity range (about 0.0 – 0.46m/s).

The bottom shear stress and suspension capacity is computed from the simulation results as well for better evaluating the possible morphodynamical response in the secondary channel. In terms of bottom shear stress, scenario A has the highest values, which is about maximum 0.94Pa near the inlet and maximum 0.37Pa near the outflow. Scenario E3 has the lowest bottom shear stress, which is about 0.49Pa near the inlet, 0.33Pa in the upstream outflow and 0.09Pa near the downstream outflow.

The suspension capacity suggests that the secondary channel indeed could transport more sediment during the flood than during the ebb. It also suggests that the inlet and the area near the outflow in the scenario A can suffer sedimentation since the suspension capacity has decreases sharply at these two locations. For the E scenarios, the inlet and the area near the upstream outflow have the possibility for sedimentation for the similar reason, but the downstream outflow in the natural situation tends to be kept since the suspension capacity is much lower in this region so it does not expect to have many sediment being transported here. Among all the scenarios, E3 has the lowest suspension capacity.

References

Akkerman G.J. (1993). Hydraulic Engineering Reports. Zandverdeling bij splitsingspunten: Literatuurinventarisatie voor inlaten van nevengeulen. Deltares (WL), Q1573.

Barneveld, H. J., Nieuwkamer, R. L. J., & Klaassen, G. J. (1994). Secondary channels: opportunities for and limitations of habitat restoration. Water science and technology, 29(3), 335-345.

Bi, Q., & Toorman, E. A. (2015). Mixed-sediment transport modelling in Scheldt estuary with a physics-based bottom friction law. Ocean Dynamics, 65(4), 555-587.

Coleman, J. M. (1969). Brahmaputra River: channel processes and sedimentation. Sedimentary geology, 3(2-3), 129-239.

IMDC (2019, in prep) Ebb-flood channel system at the Upper Sea Scheldt (Wijmeers). Document I/NO/11448/18.231/EKR/GVH. Antwerp, Belgium

Kleinhans, M. G., & van den Berg, J. H. (2011). River channel and bar patterns explained and predicted by an empirical and a physics-based method. Earth Surface Processes and Landforms, 36(6), 721-738.

Maity, S. K., & Maiti, R. (2017). Sedimentation in the Rupnarayan River: Volume 1: Hydrodynamic Processes Under a Tidal System. Springer.

Robinson, A. H. W. (1960). Ebb-flood channel systems in sandy bays and estuaries. Geography, 45(3), 183-199.

Schropp, M. H. I. (1995). Principles of designing secondary channels along the River Rhine for the benefit of ecological restoration. Water Science and Technology, 31(8), 379-382.

Smolders, S.; Maximova, T.; Vanlede, J.; Plancke, Y.; Verwaest, T.; Mostaert, F. (2016). Integraal plan Boven-Zeeschelde: Subreport 1. SCALDIS: a 3D Hydrodynamic model for the Scheldt Estuary. Version 5.0. WL Rapporten, 13_131. Flanders Hydraulics Research: Antwerp. XXVIII, 246 + 228 p. bijl. pp.

Toorman, E.A. (2000). Numerical simulation of turbulence damping in sediment-laden flow. Part 2. Suspension capacity of uniform turbulent shear flows. Report HYD/ET/00/COSINUS4, Hydraulics Laboratory, K.U.Leuven, 23pp.

Van Veen, J. (1950). Eb en vloedschaar systemen in de Nederlandse getijwateren. Tijdschrift Koninklijk Nederlandsch Aardrijkskundig Genootschap, 67, 303-325.

Winterwerp, J. C., & Van Kesteren, W. G. (2004). Introduction to the physics of cohesive sediment dynamics in the marine environment (Vol. 56). Elsevier.

Appendix: Steering file of the Wijmeers model

```
/----------------------------------------------------------------------/
/                   TELEMAC3D Version v7p3                             /
/----------------------------------------------------------------------/

TITLE = 'Wijmeers model'
PARALLEL PROCESSORS = 12

/----------------------------------------------------------------------/
/                         INPUT-OUTPUT, FILES                          /
/----------------------------------------------------------------------/

GEOMETRY FILE            = 'geo_vloedschaar_wijmeers_v3.slf'
BOUNDARY CONDITIONS FILE = 'bc_vloedschaar_wijmeers_v3.cli'
LIQUID BOUNDARIES FILE   = 'lbd_vloedschaar_wijmeers.txt'
FORTRAN FILE             = 'user_fortran'

2D RESULT FILE           = 'r2D_vloedschaar_wijmeers.slf'
3D RESULT FILE           = 'r3D_vloedschaar_wijmeers.slf'

/----------------------------------------------------------------------/
/            INPUT-OUTPUT,TIME STEP, GRAPHICS AND LISTING              /
/----------------------------------------------------------------------/

TIME STEP             = 5.0
NUMBER OF TIME STEPS  = 691200   /40 days

NUMBER OF FIRST TIME STEP FOR GRAPHIC PRINTOUTS   = 0
NUMBER OF FIRST TIME STEP FOR LISTING PRINTOUTS   = 0
GRAPHIC PRINTOUT PERIOD   = 120
LISTING PRINTOUT PERIOD   = 120
VARIABLES FOR 2D GRAPHIC PRINTOUTS  = U,V,S,H,US,TA*
VARIABLES FOR 3D GRAPHIC PRINTOUTS  = Z,U,V,W,K,EPS,TA*

ORIGINAL DATE OF TIME     = 2013;07;31
ORIGINAL HOUR OF TIME     = 22;20;00

MASS-BALANCE     = YES
INFORMATION ABOUT MASS-BALANCE FOR EACH LISTING PRINTOUT = YES

/----------------------------------------------------------------------/
/                              FRICTION                                /
/----------------------------------------------------------------------/

LAW OF BOTTOM FRICTION                  = 4
FRICTION COEFFICIENT FOR THE BOTTOM     = 0.02

LAW OF FRICTION ON LATERAL BOUNDARIES   = 5  / Nikuradse Law
FRICTION COEFFICIENT FOR LATERAL SOLID BOUNDARIES  = 0.01

/----------------------------------------------------------------------/
/                 EQUATIONS, BOUNDARY CONDITIONS                       /
/----------------------------------------------------------------------/

VELOCITY PROFILES            = 1;1
PRESCRIBED FLOWRATES         = 0.0;0.0 / read from liquid boundary file
```

```
PRESCRIBED ELEVATIONS        = 0.0;0.0
OPTION FOR LIQUID BOUNDARIES = 1;1

/-----------------------------------------------------------------/
/                EQUATIONS, INITIAL CONDITIONS                    /
/-----------------------------------------------------------------/

NUMBER OF HORIZONTAL LEVELS   = 6
MESH TRANSFORMATION           = 1 /sigma transformation

INITIAL CONDITIONS            = 'CONSTANT ELEVATION'
INITIAL ELEVATION             = 3.19602465629578

/-----------------------------------------------------------------/
/                              TURBULENCE                         /
/-----------------------------------------------------------------/

HORIZONTAL TURBULENCE MODEL                          = 4
VERTICAL TURBULENCE MODEL                            = 2
COEFFICIENT FOR HORIZONTAL DIFFUSION OF VELOCITIES   = 1.E-6
COEFFICIENT FOR VERTICAL DIFFUSION OF VELOCITIES     = 1.E-6

OPTION FOR THE BOUNDARY CONDITIONS OF K-EPSILON = 2

MIXING LENGTH MODEL    = 3 / in case of using ML model
/DAMPING FUNCTION       = 3  / in case of using ML model

/-----------------------------------------------------------------/
/                              CORIOLIS                           /
/-----------------------------------------------------------------/

CORIOLIS                 = YES
CORIOLIS COEFFICIENT     = 1.13522E-04

/-----------------------------------------------------------------/
/                       TIDAL FLATS                               /
/-----------------------------------------------------------------/

TIDAL FLATS                                  = YES

OPTION FOR THE TREATMENT OF TIDAL FLATS      = 1
TREATMENT OF NEGATIVE DEPTHS                 = 1
MINIMAL VALUE FOR DEPTH                      = 0.002

THRESHOLD FOR VISCOSITY CORRECTION ON TIDAL FLATS = 0.002
BYPASS VOID VOLUMES = NO

/-----------------------------------------------------------------/
/                           WIND                                  /
/-----------------------------------------------------------------/

WIND                               = NO
OPTION FOR WIND                    = 2
COEFFICIENT OF WIND INFLUENCE      = 0.565E-6

/-----------------------------------------------------------------/
/                           TRACERS                               /
/-----------------------------------------------------------------/

NUMBER OF TRACERS           = 0
/NAMES OF TRACERS            = 'SALINITY        PSU             '
```

```
/INITIAL VALUES OF TRACERS   = 0
/PRESCRIBED TRACERS VALUES   = 0.1;34

/AVERAGE WATER DENSITY       = 1025
/DENSITY LAW                 = 2 /variation according to salinity

/COEFFICIENT FOR VERTICAL DIFFUSION OF TRACERS   =1.E-6
/COEFFICIENT FOR HORIZONTAL DIFFUSION OF TRACERS =1.E-6

/TREATMENT OF FLUXES AT THE BOUNDARIES = 1;1
/TRACERS VERTICAL PROFILES = 1;1

/-----------------------------------------------------------------------/
/ SEDIMENT TRANSPORT
/-----------------------------------------------------------------------/

/SEDIMENT = NO
/COHESIVE SEDIMENT = YES

/MEAN DIAMETER OF THE SEDIMENT = 0.00005
/DENSITY OF THE SEDIMENT = 2650.0
/CONSTANT SEDIMENT SETTLING VELOCITY = 0.5E-3
/HINDERED SETTLING = NO

/BED LAYERS THICKNESS = 0.0
/NUMBER OF SEDIMENT BED LAYERS = 1

/INITIAL THICKNESS OF SEDIMENT LAYERS = 0.0
/MUD CONCENTRATIONS PER LAYER = 500

/EROSION COEFFICIENT = 3.0E-4
/CRITICAL EROSION SHEAR STRESS OF THE MUD LAYERS = 0.1
/CRITICAL SHEAR STRESS FOR DEPOSITION = 1000.0

/THRESHOLD FOR SEDIMENT FLUX CORRECTION ON TIDAL FLATS = 0.1

/ADVECTION-DIFFUSION SCHEME WITH SETTLING VELOCITY = 0

/SOLVER FOR DIFFUSION OF THE SEDIMENT          = 1
/ACCURACY FOR DIFFUSION OF SEDIMENT            = 1.E-6
/MAXIMUM NUMBER OF ITERATIONS FOR DIFFUSION OF SEDIMENT = 105
/PRECONDITIONING FOR DIFFUSION OF THE SEDIMENT = 2


/-----------------------------------------------------------------------/
/                          NUMERICAL SETUP                              /
/-----------------------------------------------------------------------/

NON-HYDROSTATIC VERSION   = NO

SUPG OPTION               = 1;0;1;1

/ The following keywords to be used with NON-HYDROSTATIC VERSION

SOLVER FOR VERTICAL VELOCITY                        = 1
MAXIMUM NUMBER OF ITERATIONS FOR VERTICAL VELOCITY  = 103
ACCURACY FOR VERTICAL VELOCITY                      = 1.E-6
PRECONDITIONING FOR VERTICAL VELOCITY               = 2

SOLVER FOR PPE                                      = 1
```

```
MAXIMUM NUMBER OF ITERATIONS FOR PPE                = 104
ACCURACY FOR PPE                                    = 1.E-6
PRECONDITIONING FOR PPE                             = 2

/---------------------------------------------------------------------/
/                          ADVECTION                                  /
/---------------------------------------------------------------------/

ADVECTION STEP                        = YES

SCHEME FOR ADVECTION OF VELOCITIES    = 1
SCHEME FOR ADVECTION OF DEPTH         = 5
SCHEME FOR ADVECTION OF TRACERS       = 1
SCHEME FOR ADVECTION OF K-EPSILON     = 1

NUMBER OF SUB ITERATIONS FOR NON LINEARITIES    = 1

/---------------------------------------------------------------------/
/                          DIFFUSION                                  /
/---------------------------------------------------------------------/

SCHEME FOR DIFFUSION OF VELOCITIES              = 1  /default implicit (0 value
cancels diffusion)
SCHEME FOR DIFFUSION OF TRACERS                 = 1
SCHEME FOR DIFFUSION OF K-EPSILON               = 1

/---------------------------------------------------------------------/
/                        PROPAGATION                                  /
/---------------------------------------------------------------------/

LINEARIZED PROPAGATION                          = NO
MEAN DEPTH FOR LINEARIZATION                    = 0

FREE SURFACE GRADIENT COMPATIBILITY             = 0.9     /only used with wave
equation
DYNAMIC PRESSURE IN WAVE EQUATION               = NO

/---------------------------------------------------------------------/
/                     NUMERICAL PARAMETERS                            /
/---------------------------------------------------------------------/

IMPLICITATION FOR VELOCITIES      = 1
IMPLICITATION FOR DEPTH           = 0.55
IMPLICITATION FOR DIFFUSION       = 1

SOLVER FOR DIFFUSION OF VELOCITIES   = 1
SOLVER FOR PROPAGATION               = 1
SOLVER FOR DIFFUSION OF TRACERS      = 1
SOLVER FOR DIFFUSION OF K-EPSILON    = 1

ACCURACY FOR DIFFUSION OF VELOCITIES = 1.E-6
ACCURACY FOR PROPAGATION             = 1.E-6
ACCURACY FOR DIFFUSION OF TRACERS    = 1.E-6
ACCURACY FOR DIFFUSION OF K-EPSILON  = 1.E-6

MAXIMUM NUMBER OF ITERATIONS FOR DIFFUSION OF VELOCITIES = 101
MAXIMUM NUMBER OF ITERATIONS FOR PROPAGATION             = 201
MAXIMUM NUMBER OF ITERATIONS FOR DIFFUSION OF TRACERS    = 102
MAXIMUM NUMBER OF ITERATIONS FOR DIFFUSION OF K-EPSILON  = 202
MAXIMUM NUMBER OF ITERATIONS FOR ADVECTION SCHEMES       = 20 /for schemes 13
and 14
```

```
PRECONDITIONING FOR DIFFUSION OF VELOCITIES   = 2
PRECONDITIONING FOR PROPAGATION               = 2
PRECONDITIONING FOR DIFFUSION OF K-EPSILON     = 2
PRECONDITIONING FOR DIFFUSION OF TRACERS      = 2

/ the higher to 1 the mass lumping parameter the more diagonal
/ the result matrix and the faster the computation, but the more the results are
smoothened
MASS-LUMPING FOR DEPTH         = 1
MASS-LUMPING FOR VELOCITIES    = 1
MASS-LUMPING FOR DIFFUSION     = 1

INITIAL GUESS FOR DEPTH        = 1

MATRIX STORAGE                 = 3

VELOCITY PROJECTED ON SOLID LATERAL BOUNDARIES = YES
VELOCITY PROJECTED ON BOTTOM                   = YES

&FIN
```

DEPARTMENT **MOBILITY & PUBLIC WORKS**
Flanders hydraulics Research

Berchemlei 115, 2140 Antwerp
T +32 (0)3 224 60 35
F +32 (0)3 224 60 36
waterbouwkundiglabo@vlaanderen.be
www.flandershydraulicsresearch.be